European Journal of Medicinal Chemistry 51 (2012) 110–123

Contents lists available at SciVerse ScienceDirect

European Journal of Medicinal Chemistry

journal homepage: http://www.elsevier.com/locate/ejmech

Original article

Studies on gambogic acid (IV): Exploring structure–activity relationship with IκB kinase-beta (IKKβ)

Haopeng Sun [a,b,1], Feihong Chen [a,c,1], Xiaojian Wang [b], Zongliang Liu [a,b], Qian Yang [b], Xiaojin Zhang [a,b], Jia Zhu [a,b], Lei Qiang [a,c], Qinglong Guo [a,c,**], Qidong You [a,b,c,*]

[a] State Key Laboratory of Natural Medicines, China Pharmaceutical University, China
[b] School of Pharmacy, China Pharmaceutical University, Nanjing 210009, China
[c] Jiangsu Key Laboratory of Carcinogenesis and Intervention, China Pharmaceutical University, Tongjiaxiang 24, Nanjing 210009, China

ARTICLE INFO

Article history:
Received 14 March 2011
Received in revised form
14 February 2012
Accepted 14 February 2012
Available online 3 March 2012

Keywords:
IKKβ
NF-κB signaling pathway
Caged xanthone
Pharmacophoric motif
Inhibitor

ABSTRACT

Previously we have reported a series of gambogic acid's analogs and have identified a compound that possessed comparable *in vitro* growth inhibitory effect as gambogic acid. However, their target protein as well as the key pharmacophoric motifs on the target have not been identified yet. Herein we report that gambogic acid and its analogs inhibit the activity of IκB Kinase-beta (IKKβ) through suppressing the activation of TNFα/NF-κB pathway, which in turn induces A549 and U251 cell apoptosis. IKKβ can serve as one of gambogic acid's targets. The preparation of the compounds was carefully discussed in the article. Caged 4-oxa-tricyclo[4.3.1.0^{3,7}]dec-2-one xanthone, which was identified as the pharmacophoric scaffold, represents a promising therapeutic agent for cancer and useful probe against NF-κB pathway.

1. Introduction

Caged *Garcinia* xanthones, a special category of polyprenylated xanthones which are naturally discovered in Garcinia plants, have received increasing attention among phytochemical, pharmacological, synthetic, and biological communities in recent years because of their potent bioactivity and unique 4-oxa-tricyclo [4.3.1.0^{3,7}]dec-2-one scaffold, in which a highly substituted tetrahydrofuran core [1,2]. Among these noticeable natural products, gambogic acid (GA, Fig. 1) is one of the best representatives. Previous studies showed that GA possessed strong growth inhibitory effect against a broad panel of cancer cell lines with IC_{50} ranging from 1 to 5 μM [3–6]. Due to its prominent growth inhibitory effect and good tolerance in different animal tests, GA has been approved by the Chinese State Food and Drug Administration (SFDA) to enter phase II clinical trial [7]. However, the mechanism of GA's anti-tumor activities is still debatable. Multiple mechanisms have been proposed by research groups worldwide, such as apoptosis induction [8], cell cycle regulation [9], telomerase depression [10,11], angiogenesis inhibition [12], reactive oxygen species (ROS) generation [13] etc. Wang *et al.* reported a comprehensive proteome profiling which deduced STMN1 as the target of GA [14]. Very recent studies further reported that GA inhibited NF-κB signaling pathway [15,16] and induced apoptosis through its interaction with the transferrin receptor [17].

As a transcription factor, NF-κB participates in the regulation of diverse biological processes, including immune, inflammatory and apoptotic response [18–20]. Under normal conditions, NF-κB binds to its natural inhibitory protein, IκBα and locates at cytoplasm. In response to an activation signal, the IκBα subunit is phosphorylated at serine residues 32 and 36, ubiquitinated at lysine residues 21 and 22, and then degraded through the ubiquitin-proteasome pathway, thus exposing the nuclear localization signals on the p50-p65 heterodimer. The p65 is then phosphorylated, leading to nuclear translocation. It binds to a specific sequence in DNA, which in turn results in gene transcription. The phosphorylation of IκBα is catalyzed by IκB kinase (IKKs), which is essential for NF-κB activation. IKKs consists of 3 subunits named IKKα, IKKβ, and IKKγ (also called NEMO). Gene deletion studies have indicated that IKKβ is the key regulator in the canonical (classical) pathway of NF-κB activation [21,22].

* Corresponding author. State Key Laboratory of Natural Medicines, China Pharmaceutical University, China. Tel./fax: +86 25 83271351.
** Corresponding author. Jiangsu Key Laboratory of Carcinogenesis and Intervention, China Pharmaceutical University, Tongjiaxiang 24, Nanjing 210009, China. Tel./fax: +86 25 83271440.
E-mail addresses: anticancerdrug@yahoo.cn (Q. Guo), youqidong@gmail.com (Q. You).
[1] These two authors contributed equally to this work.

0223-5234/$ – see front matter © 2012 Elsevier Masson SAS. All rights reserved.
doi:10.1016/j.ejmech.2012.02.029

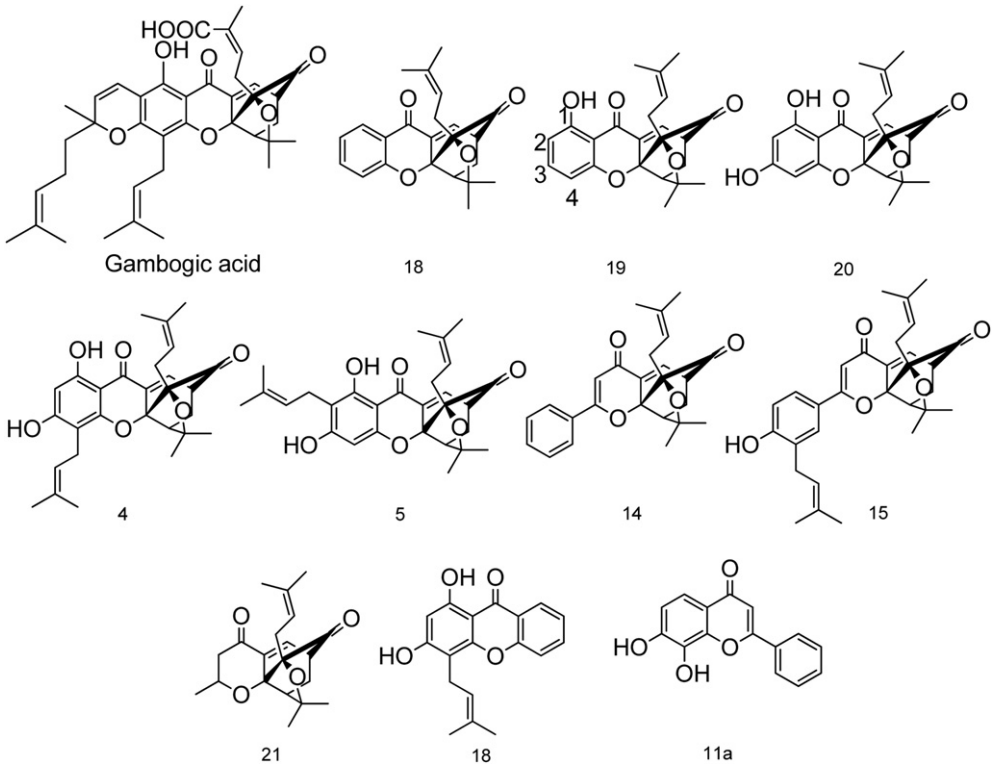

Fig. 1. The structure of gambogic acid (GA) and ten designed derivates.

Several strategies focusing on the modification of GA have already been reported [23,24]. Previously, we have reported a series of GA's analogs and discovered the importance of "caged" xanthones for the growth inhibitory effect through a strict "step by step" modification strategy [24]. Among these analogs, compound **19** (Fig. 1) possessed comparable *in vitro* growth inhibitory effect as GA, while its chemical structure was remarkably simplified. However, the mechanism by which GA and its analogs exert their anti-tumor effects, particularly their target protein, remains to be clarified. Considering that previously suggested targets such as telomerase, CDK7 and STMN1 are all client proteins of NF-κB signaling pathway, in the present study, we tried to identify the key regulator of NF-κB signaling pathway affected by GA and its analogs. Our results suggested that GA inhibited the activation of NF-κB signaling pathway through suppression the activity of IKKβ and further induced the apoptosis of A549 and U251 cancer cell lines. Furthermore, because of the complexed structure and huge difficulties in total synthesis of GA, we tried to identify the pharmacophoric motif of GA to inhibit IKKβ using the same strategy described in our previous paper [24]. The 4-oxa-tricyclo[4.3.1.$0^{3,7}$] dec-2-one was certified to be the key scaffold of GA to exert its inhibition effect on IKKβ. Additionally, we also studied the effects of the substituents such as hydroxyl and isopentenyl groups. Mechanistic studies for the most potent compound **20** showed that it possessed a very similar mechanism with GA. Its structure provides a new skeleton for developing novel IKKβ inhibitors. It is also a promising chemical probe to understand NF-κB signaling pathway as well as the biological functions of IKKβ.

2. Results and discussion

2.1. Chemistry

In order to identify the pharmacophoric motif of GA, we designed and synthesized ten GA's analogs (Fig. 1). The synthetic route for xanthone-based caged compounds **4** and **5** were summarized in Scheme 1. Briefly, xanthone **1** was *O*-alkylated with 2-chloro-2-methyl butyne in the presence of potassium carbonate and a catalytic amount of copper iodide in acetone to afford alkyne **2**. Reduction of **2** with Lindlar catalyst produced 3,5,6-tris-(1,1-dimethyl-allyloxy)-9*H*-xanthen-9-one (**3**). The desired target compounds **4** and **5** were obtained from Claisen/Diels–Alder cascade reaction of **3** in DMF at 120 °C for 1 h.

The preparation of flavanone-based caged compounds **14** and **15** was outlined in Scheme 2. 2,3,4-trihydroxyacetophenone was selected as starting material. Benzyl bromide was employed to protect the hydroxyl groups of **6** to afford **7** in 85% yield. Selective debenzylation of the phenolic group adjacent to the ethanone moiety was achieved by the action of trifluoroacetic acid in toluene, leading to *O*-hydroxyacetophenone derivative **8** in 70% yield. Chalcone compound derivative **9a** or **9b** was prepared by condensation of **8** with benzaldehyde or 4-benzyloxy benzaldehyde, respectively. **10a** or **10b** was obtained by cyclization of **9a** or **9b** in a solution of DMSO at 110 °C in ~70% yield. Deprotection of benzyl groups using 10% Pd/C in THF/CH_3OH led to **11a** or **11b**. The resulted flavones were then *O*-alkylated with 2-chloro-2-methyl butyne and reduced with Lindlar catalyst to produce **13a** and **13b**. The desired targeted compound **14** or **15** was obtained from Claisen/Diels–Alder cascade reaction of **13a** or **13b** in DMF at 120 °C for 1 h.

The preparation of **17** was described in Scheme 3. Compound **16** was obtained through the condensation of phloroglucinol and salicylic acid mediated by $ZnCl_2$ in $POCl_3$ in 43% yield. It was then alkylated with isopentenyl bromide in the condition of $NaOCH_3$ and CH_3OH in 11% yield.

The preparation of flavanone-based caged compounds **20** was outlined in Scheme 4. Xanthone **24** was obtained from xanthone **1** via selective protection of 5,6-bihydroxyl with Ph_2CCl_2, 3-hydroxyl with MOMCl (Methyl chloromethyl ether) and 1-hydroxyl with Ac_2O in 76% yield over three steps. Deprotection of the 5,6-biphenyl group via hydrogenolysis at the presence of Pd/C (95%) lead to compound **25**.

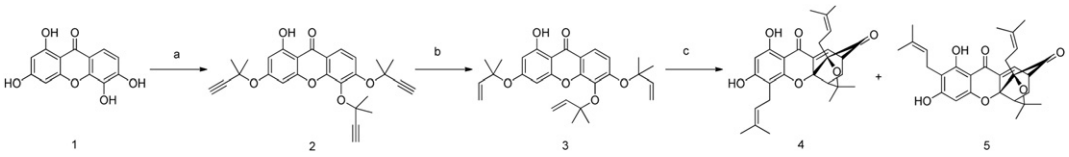

Scheme 1. The synthetic route for compound **4** and **5**. *Reagents and conditions*: (a) $ClC(CH_3)_2C{\equiv}CH_2$, K_2CO_3, KI, CuI, CH_3COCH_3, 50 °C, 5 h; (b) 10% Pd/$BaSO_4$, $CH_3COOC_2H_5/C_2H_5OH$ (1:3, v/v), rt, 2 h; (c) DMF, 120 °C, 1 h.

5,6-dihydroxy groups were alkylated simultaneously with 2-chloro-2-methyl butyne in the presence of KI and K_2CO_3 under CuI catalysis in 70% yield and lead to compound **26**. Compound **27** was easily formed from compound **26** via hydrogenolysis at the presence of Pd/$BaSO_4$ and Claisen/Diels–Alder cascade reaction in 65% yield over two steps. Caged compound **20** was obtained via deprotection of Ac and MOM groups simultaneously under the condition of 3 M HCl in acetone with the yield of 60%.

Compound **18**, **19** and **21** was synthesized using the method previously reported by our laboratory [24].

2.2. GA inhibits TNF-induced phosphorylation and nuclear translocation of p65

In response to an activation signal, the IκBα subunit is phosphorylated at serine residues 32 and 36, then ubiquitinated at lysine residues 21 and 22, and degraded through the proteasomal pathway, thus exposing nuclear localization signals on the NF-κB, leading to its interaction with a specific sequence in DNA, which in turn results in gene transcription [15]. Suppression of NF-κB signaling should inhibit the translocation of p65 to the nucleus. We first investigated the effect of GA on TNFα induced NF-κB nuclear translocation by using high content screening. The results confirmed that GA suppressed the translocation of NF-κB to the nucleus (Fig. 2A). GA dose-dependently inhibited TNFα induced NF-κB nuclear translocation, with 50.2% inhibition at 5 μM (Fig. 2B).

We also determined the effect of GA on TNFα induced nuclear translocation of p65 by Western blot analysis. GA obviously suppressed TNFα induced translocation of p65 in a dose-dependent manner (Fig. 3).

2.3. GA inhibits TNF-dependent IκBα degradation and phosphorylation

The translocation of NF-κB to the nucleus is preceded by the phosphorylation, ubiquitination, and proteolytic degradation of IκBα. To determine whether inhibition of TNFα-induced NF-κB translocation was due to inhibition of IκBα degradation, cells were pretreated with 4 or 8 μM GA and then exposed to TNFα for various time periods. We then examined the IκBα degradation in the

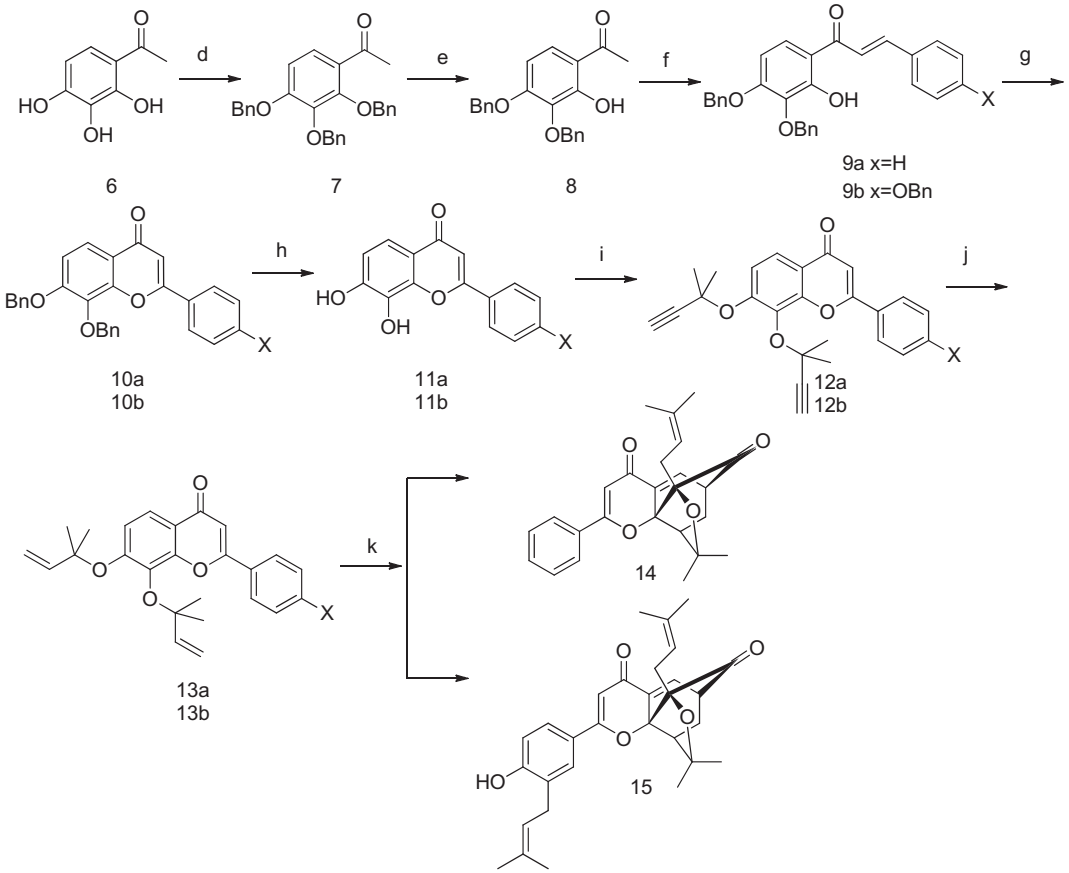

Scheme 2. The synthetic route for compound **11a**, **14** and **15**. *Reagents and conditions*: (d) BnBr, K_2CO_3, KI, DMF, 50 °C, 8 h; (e) trifluoroacetic acid/toluene (1:5, v/v), rt, 1 h; (f) 20% aqueous KOH/EtOH, rt, 36 h; (g) I_2, DMSO, 110 °C, 12 h; (h) 10% Pd/C, THF/CH_3OH (1:1, v/v), rt, 3 h; (i) $ClC(CH_3)_2C{\equiv}CH_2$, K_2CO_3, KI, CuI, CH_3COCH_3, 50 °C, 4 h; (j) 10% Pd/$BaSO_4$, $CH_3COOC_2H_5/C_2H_5OH$ (1:3, v/v), rt, 2 h; (k) DMF, 120 °C, 1 h.

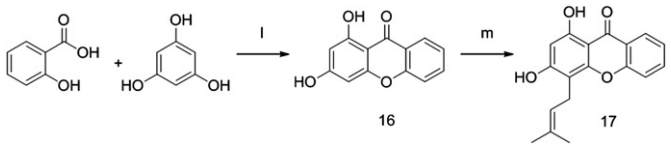

Scheme 3. The synthetic route for compound **17**. *Reagents and conditions*: (l) $ZnCl_2$, $POCl_3$, 70 °C, 3 h; (m) $BrCH_2CHC(CH_3)_2$, NaOMe, CH_3OH, rt, 12 h.

cytoplasm by Western blot analysis. TNFα induced IκBα degradation in the control cells in 15 min, but it had no effect on IκBα degradation in GA pretreated cells (Fig. 4). Moreover, the phosphorylation of IκBα was stimulated by TNFα in 15 min, and it was suppressed by GA. These results indicated that GA inhibited TNF-induced NF-κB activation through inhibition of IκBα phosphorylation and suppression of IκBα degradation.

2.4. Identification of caged 4-oxa-tricyclo[4.3.1.$0^{3,7}$]dec-2-one xanthones as a new scaffold of IKKβ inhibitor

GA is a natural product isolated from the resin of *Garcinia hanburyi*. The complicated structure of GA brings huge hindrance for its further usage. To simplify the structure skeleton and to find out the key pharmacophoric motifs that account for GA's biological function, 10 derivatives of GA were designed and synthesized (Fig. 1).

MTT assays were first performed to ascertain inhibitory effect on cell viability by GA and its derivatives in A549 and U251 cells. Following 24 h treatment, GA inhibited the viability of A549 and U251 cells and the IC_{50} value was 1.10 μM and 2.56 μM, respectively (Table 1). Compounds **19** and **20** showed equivalent *in vitro* growth inhibitory effects to GA.

Since GA inhibited the phosphorylation and degradation of IκBα, we further tested the effect of GA and its derivatives on the activity of IKKβ, an enzyme that was reported to play crucial role in IκBα degradation and NF-κB activation [25]. By using HTScan IKKβ kinase assay kit, we found that GA remarkably suppressed the activity of IKKβ. The phosphorylation of IκBα by IKKβ was inhibited by GA with IC_{50} of 3.07 μM. Additionally, compounds contained caged 4-oxa-tricyclo[4.3.1.$0^{3,7}$]dec-2-one xanthone scaffold (**4**, **5**, **18**, **19** and **20**) showed similar activity to GA (Table 1). Among all the derivatives, compound **19** and **20** showed remarkable IKKβ inhibitory effect, with IC_{50} 8.17 μM and 3.52 μM, respectively. Considering its potent cell viability inhibitory effects, we thus concluded that this structure contained the key pharmacophoric motif of GA.

To further study the mechanism of GA and its derivatives to inhibit the viability of cancer cells, we chose GA and compound **20** to study their effects on apoptosis and cell cycle distribution. The substantial morphological changes observed in GA-treated and **20**-treated U251 cells were examined and photographed by an inverted light microscope. Damaged cells became round and shrunken, while the untreated cells retained the normal size and shape (Fig. 5A). Identified by DAPI staining, the bright nuclear condensation and the apoptotic bodies appeared after treatment with **20** (Fig. 5B). To further confirm the apoptosis induced by GA and **20**, Annexin V/PI staining assay was used. After treated with 4, 8 and 16 μM **20** and 8 μM GA for 24 h, the early and median apoptotic cells (right low section of fluorocytogram) were increased (from 2.75% to 58.21%, Fig. 5C and D) and the late apoptotic and necrotic cells (right upper section of fluorocytogram) were also increased strikingly (from 1.39% to 34.24%, Fig. 5B and C). These results suggested that apoptosis induction by **20** was involved in its anti-tumor effect. **20** induced apoptosis in a very similar manner to GA, which further confirmed that **20** possessed the key pharmacophoric motifs of GA.

Based on immunofluorescence experiment, we next studied whether **20** exhibited similar mechanism to GA in inhibiting the activation of NF-κB signaling pathway. We found that **20** inhibited TNFα-induced NF-κB nuclear translocation in a dose-dependent manner (Fig. 6). This further demonstrated that **20** exhibited its anti-cancer effect in a very similar mechanism to GA.

2.5. Structure–activity relationships

To further identify the pharmacophoric motif of GA, we explored structure–activity relationships (SAR) using IKKβ kinase assay and cellular assay. Generally, compounds possessed caged 4-oxa-tricyclo[4.3.1.$0^{3,7}$]dec-2-one xanthone scaffold (**4**, **5**, **18**, **19** and **20**)

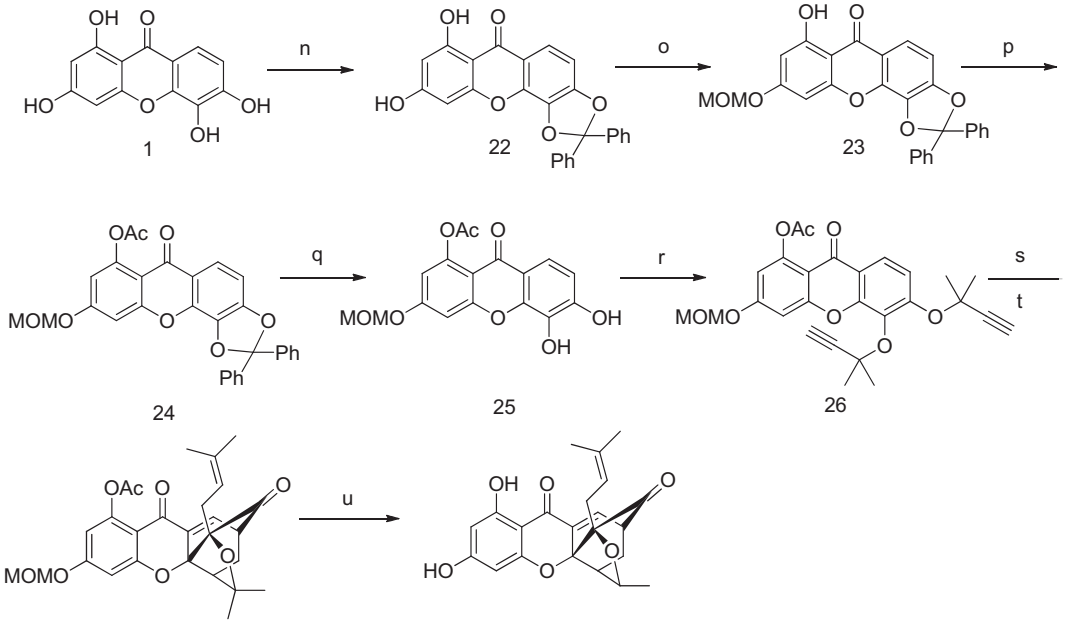

Scheme 4. The synthetic route for compound **20**. *Reagents and conditions*: (n) Ph_2CCl_2, DIPEA, Ph_2O, 170 °C, 0.5 h; (o) MOMCl, K_2CO_3, acetone, 25 °C, 5 h; (p) Ac_2O, DMAP, CH_2Cl_2, 25 °C, 4 h; (q) H_2, Pd/C, THF/MeOH, 50 °C, 12 h; (r) $(CH_3)_2CClC{\equiv}CH$, KI, K_2CO_3, CuI, acetone, reflux, 1.5 h; (s) H_2, Pd/$BaSO_4$, EtOH/EtOAc, 35 °C, 4 h; (t) DMF, 120 °C, 1 h; (u) 3M HCl, acetone, 40 °C, 6 h.

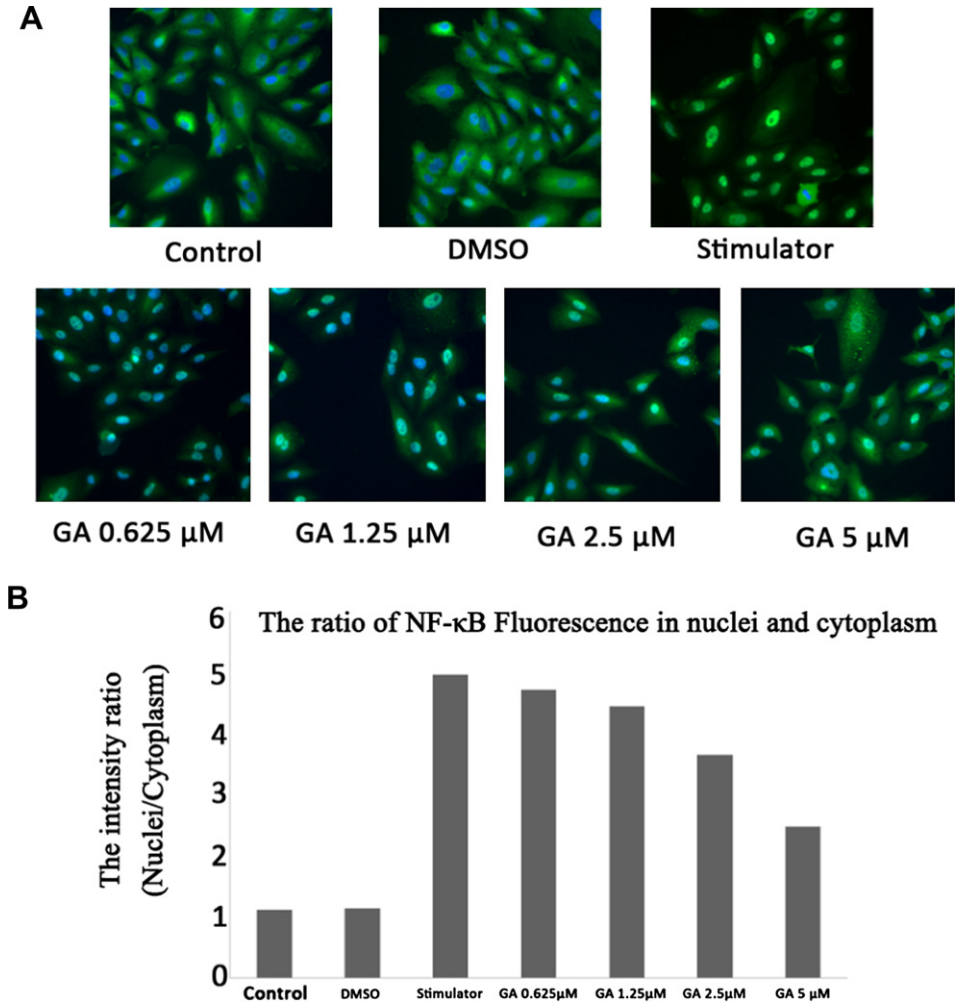

Fig. 2. High content analysis of NF-κB localization. (A) A549 cells were first treated with indicated dose of GA for 2 h at 37 °C and then exposed to mixed stimulators for 30 min. Then the cells were underwent high content analysis. (B) The ratio of NF-κB fluorescence in nuclei and cytoplasm, indicating the inhibition rate of NF-κB translocation by GA. (For interpretation of the references to color in this figure legend, the reader is referred to the web version of this article.)

exhibited similar activity to GA on not only A549 and U251 cancer cell lines but also IKKβ, indicating this scaffold was the key pharmacophoric motif of GA. The activities of compounds that were lack of either xanthone structure (**14**, **15** and **21**) or caged 4-oxa-tricyclo [4.3.1.0^{3,7}]dec-2-one ring (**11a** and **17**) remarkably decreased in both cellular and kinase test. Compound **14** and **15** with caged flavone scaffold was approximately 10–15 fold less active on kinase activity and 8–10 fold less active on cancer cells than compound **20**. Although flavone compound **11a** and xanthone compound **17** possessed moderate activity on IKKβ (3–4 fold less active than **20**), their activity on cancer cells dramatically decreased.

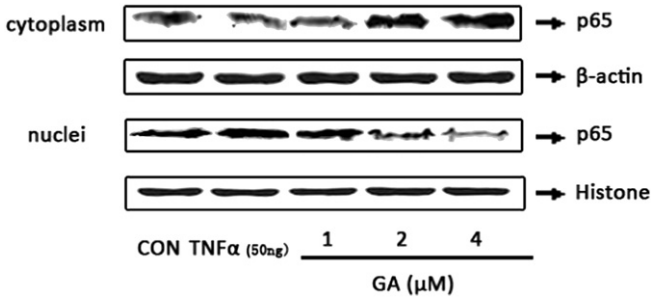

Fig. 3. GA inhibits TNFα-induced nuclear translocation of p65. A549 cells were either untreated or pretreated with indicated dose of GA for 4 h at 37 °C and then treated with 50 ng/mL TNFα for 30 min. Cytoplasmic and nuclear extracts were prepared and analyzed by western blotting with antibodies against p65. For loading control of cytoplasmic and nuclear protein, the membrane was blotted with β-actin and histone antibody, respectively.

Additionally, the substituted groups on 4-oxa-tricyclo[4.3.1.0^{3,7}] dec-2-one xanthone scaffold were also important to their activities. We have previously demonstrated that C1 hydroxy group was indispensable for the growth inhibitory effect of **19** [24]. This group was crucial for the inhibitory activity on IKKβ. Compounds possessed this group such as **19** and **20** were most effective on IKKβ, while compound lacking this group such as **18** was approximately 8-fold less active than **20**. It has been reported that the formation of H-bond interactions between inhibitors and the hinge region of IKKβ were very important [26]. The missing of hydroxy groups in **18** might cause the decrease in its activity. The results also verified the importance of hydroxy groups in this series of compounds. The activities of compound **4** and **5** on both cancer cell lines and IKKβ enzyme were a little bit lower than **19** and **20**. These results suggested that the isopentenyl motif on the phenyl ring of these compounds was not necessary for the bioactivity, removal of this motif would not affect the inhibitory effect, and thus would simplify the structure.

We also compared the most potent compounds **19** and **20**. **20** possessed a C3 hydroxy group. Although it did not affect the activity remarkably, more modifications such as O-alkylation could be

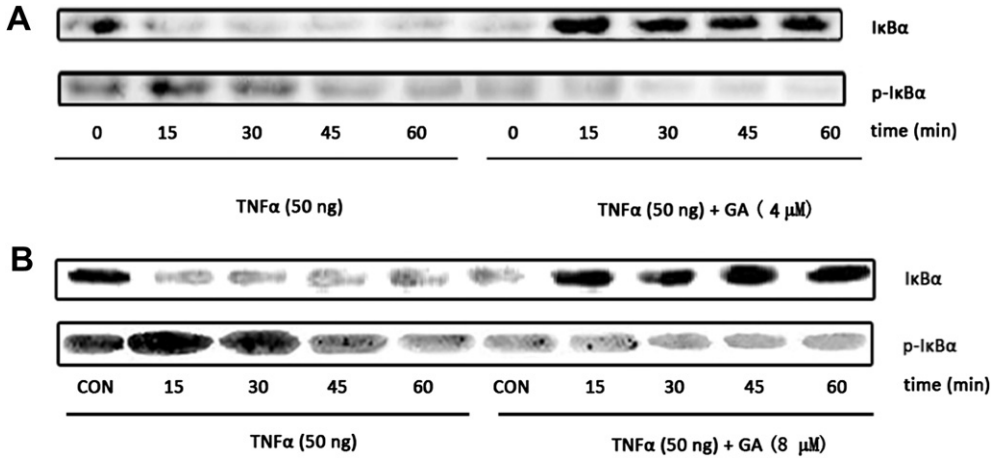

Fig. 4. Effect of GA on TNFα-induced degradation of IκBα. A549 cells were incubated with 4 μM (A) and 8 μM (B) GA for 4 h and treated with 0.1 ng/mL TNF for the indicated times. Cytoplasmic extracts were prepared and analyzed by western blotting with antibodies against IκBα and phorspho-IκBα.

carried out on this position, and thus might lead to more potent molecules. Additionally, this group might also enhance the solubility of the caged xanthone compounds and improve the physicochemical properties.

In summary, (a) caged 4-oxa-tricyclo[4.3.1.0^{3,7}]dec-2-one xanthone scaffold was the key pharmacophoric motif of GA, (b) this scaffold possessed potent inhibitory effect on cancer cell proliferation and similar molecular mechanism to GA, (c) this scaffold could serve as a new skeleton of IKKβ inhibitor, (d) hydroxy groups on this scaffold especially at C1 position enhanced the IKKβ inhibitory effect, while the isopentenyl group at the aromatic ring was not important.

2.6. Molecular binding pattern study of GA and its derivatives with IKKβ by molecular docking

To further illustrate the binding mode of IKKβ with its inhibitors, we built up the protein homology model of IKKβ [27]. Previously work has demonstrated that GA covalently modified IKKβ at Cys179 [16]. However, the MS analysis of this modification was based on a short peptide around the binding site of IKKβ, it was not clear whether the spatial structure of this peptide was in accord with the "real" structure under physiological environment. No crystal structure has been reported until now. As a result, the computational method is meaningful and can help us to form a deeply insight into the binding patterns of this series of compounds with IKKβ. The binding modes were studied using the docking program Gold 3.0. Gold score Fitness was selected to evaluate the binding affinity (Table 2). By analyzing the data, it was evident that the Glodscore Fitnesses of most compounds were in well correlation with the experimental data, indicating that the model was reliable for binding mode study. GA, compound **14**, **20** and **21** were taken as examples to depict the binding mode (Fig. 7). All 4 compounds could located in the ATP binding pocket of IKKβ and make several H-bonds with the hinge region of the enzyme, which is considered to be a common binding pattern of IKKβ and its inhibitors [28–33]. To be more specific, GA formed H-bonds with Asp103 and Lys106, compound **20** formed H-bonds with Cys99 and Lys106. However, compound **14** and **21** only formed one H-bond with Lys106, which may explain the decrease of their IKKβ inhibitory activity as well as the anti-tumor effect. Our results agreed with Nagarajan *et al.* in that as the key residues within the ATP binding pocket of IKKβ, Cys99 and Asp103 could form H-bond with ATP and frequently interact with the inhibitors [26]. Besides, there are 3 hydrophobic pockets (Fig. 7) in the binding site of IKKβ. P1 is formed by Leu21, Gly22, Thr23 and Lys46, P2 is formed by Met96, Cys99, Ile165 and Glu172, P3 is formed by Asp103, Glu149 and Asn150 [26]. As depicted in Fig. 7, GA occupied P1 and P3 (Fig. 7D), **14** and **20** occupied P2 and P3 (Fig. 7A and B, respectively), while **21** obviously missed P1 and P2. The result indicated a lower binding affinity of this compound, and explained the decrease of the inhibitory effect.

Very recently, the co-crystal structure was reported by Xu, G. *et al* [41]. We compared the binding pattern of GA with homology model (Fig. 8A) to the pattern with the crystal structure (PDB id: 3QAD, Fig. 8B). We can see that the two binding model were very similar. In both patterns, GA formed H-Bond with Asp103 and Lys106. Asn109 and Glu149 were also important for GA's binding. Compared to the co-crystal structure, GA located well in the ATP binding pocket of IKKβ. Previous study indicated that GA covalently bind to Cys179 (Fig. 8B). However, this residue obviously locates at the edge loop region of IKKβ, which not correlate to the ATP binding pocket. It needs to be emphasize that Cys99, a residue located at the ATP binding pocket of IKKβ, has been mentioned to be crucial for the activity of IKKβ. The double bond at isopentenyl group of GA is close to this residue, indicating the possibility of covalent binding. Thus, it may be Cys99, not Cys179, that contributes to the covalent binding of GA with IKKβ.

Table 1
Inhibition of IKKβ and cell proliferation by GA and its analogs.

Comp.	IKKβ IC_{50} (μM)	A549 IC_{50} (μM)	U251 IC_{50} (μM)
4	6.60	3.58	8.57
5	10.78	14.41	22.44
11a	9.82	37.25	50.11
14	41.65	27.46	40.24
15	25.30	15.51	18.74
17	13.14	34.89	46.76
18	24.16	1.93	18.70
19	8.17	0.70	9.05
20	3.52	2.67	7.32
21	40.27	60.26	82.43
GA	3.07	1.10	2.56

3. Conclusion

Inspired by the previous study by our group [24] and the molecular mechanism research of GA on NF-κB pathway described by Pandey, Ujjawal and colleagues [15,16], we verified that the anti-tumor effects of GA were mediated through modulation of the NF-κB pathway and IKKβ was confirmed as the the key regulator of the pathway affected by GA. However, the complicated structure of

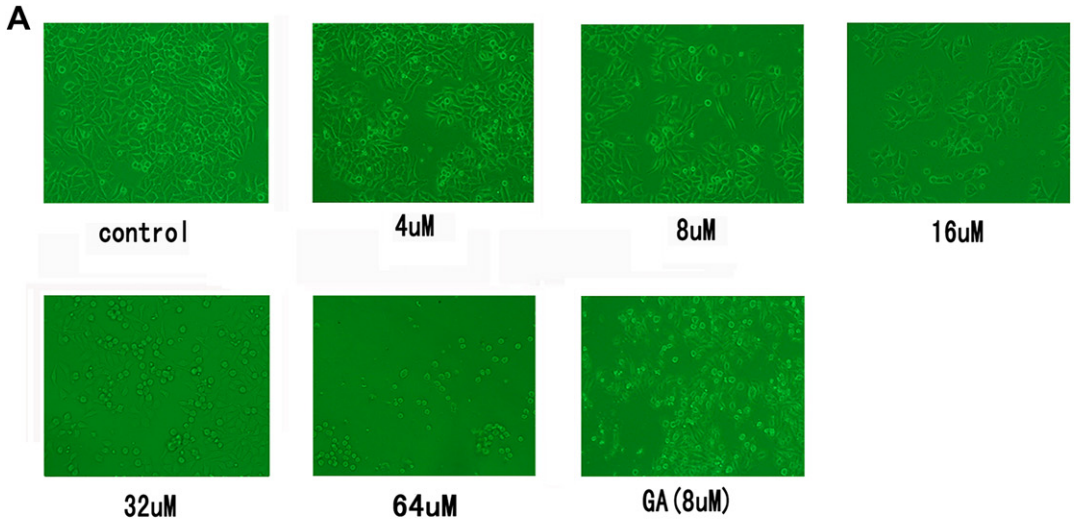
A
control
4uM
8uM
16uM
32uM
64uM
GA (8uM)

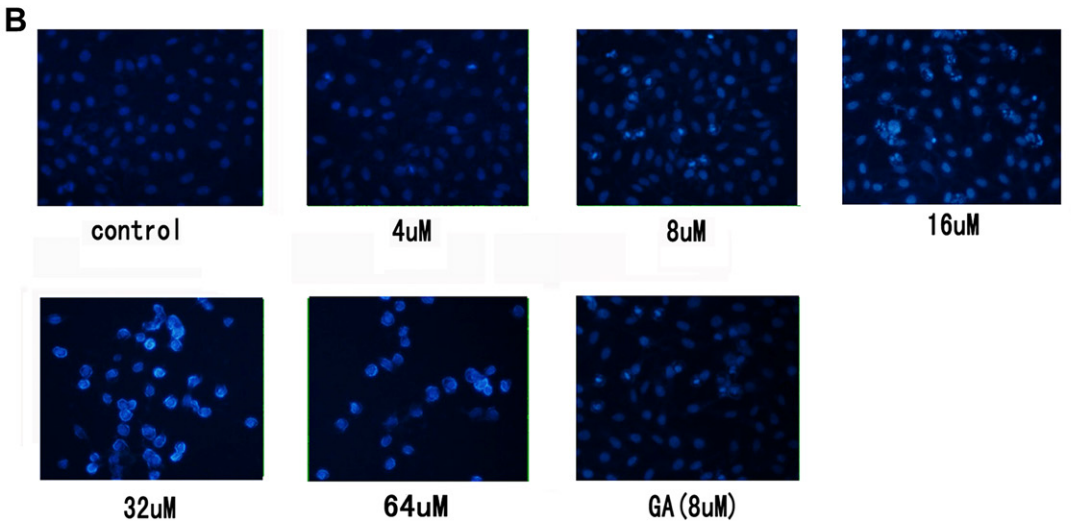
B
control
4uM
8uM
16uM
32uM
64uM
GA (8uM)

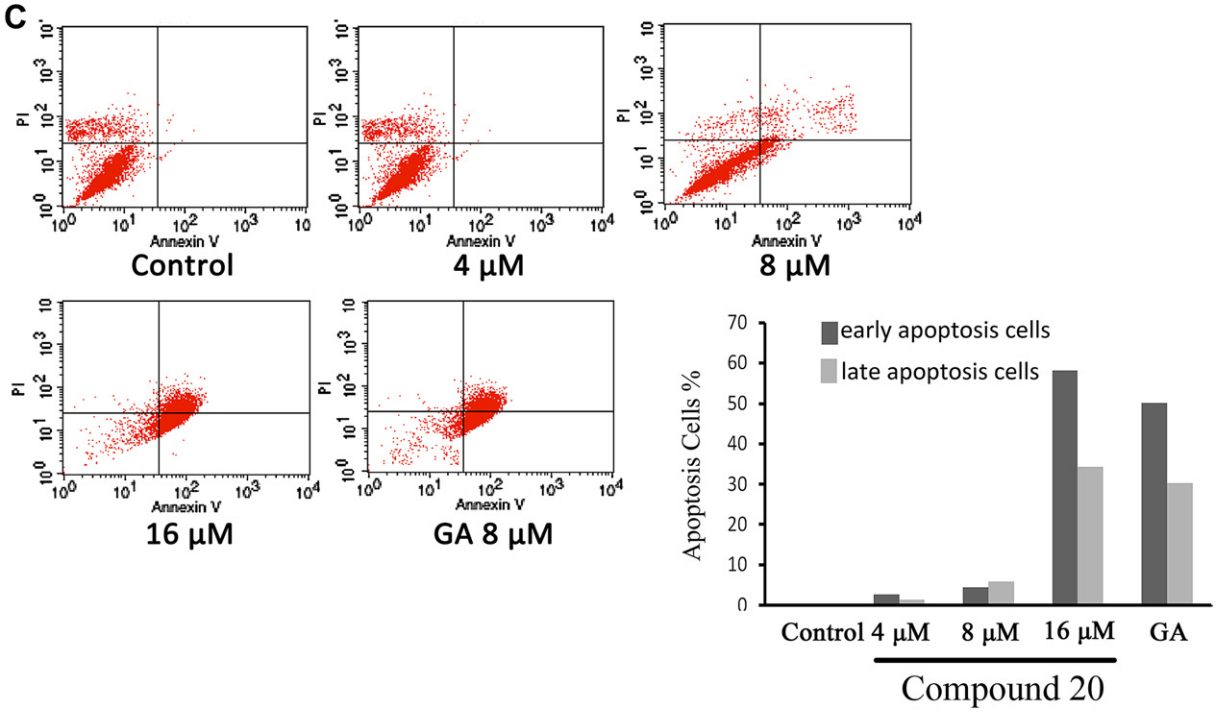
C
PI
Annexin V
Control
4 μM
8 μM
16 μM
GA 8 μM
Apoptosis Cells %
early apoptosis cells
late apoptosis cells
Control 4 μM 8 μM 16 μM GA
Compound 20

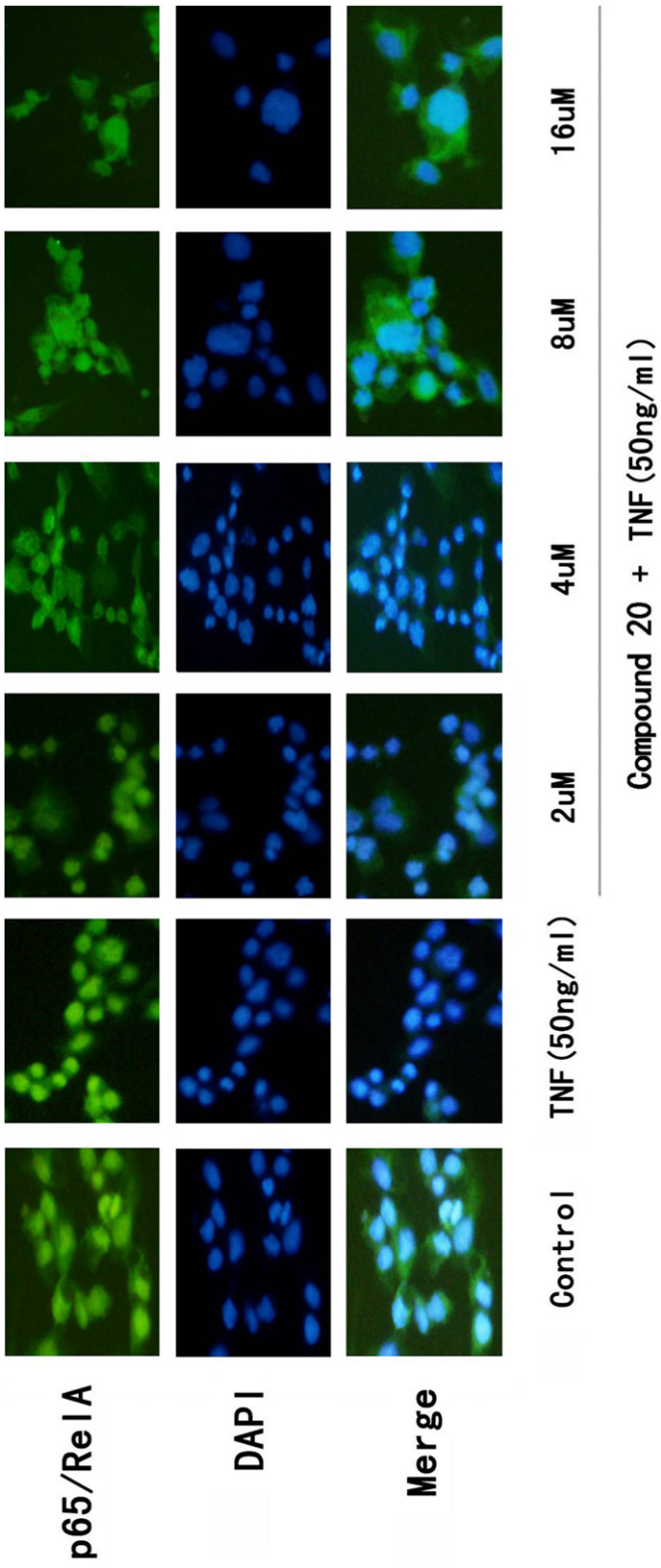

Fig. 6. Immunofluorescence staining for Rel A (p65) and nucleus in U251 cells: green represents p65, blue represents nuclei, and merge represents both. (For interpretation of the references to color in this figure legend, the reader is referred to the web version of this article.)

Table 2
The binding information of GA and its analogs with IKKβ protein homology model.

Compound	Gold Score	IKKβ IC_{50} (μM)
4	59.46	6.60
5	54.25	10.78
11a	48.87	9.82
14	41.21	41.65
15	49.20	25.30
17	50.22	13.14
18	46.67	24.16
19	54.57	8.17
20	57.67	3.52
21	38.75	40.27
GA	60.46	3.07

GA brings huge hindrance for its further usage. To simplify the structure skeleton and to find out the key pharmacophoric motifs that account for GA's biological function, ten derivatives of GA were synthesized and evaluated for their inhibitory effect on IKKβ as well as cancer cell proliferation. The caged 4-oxa-tricyclo[4.3.1.$0^{3,7}$]dec-2-one xanthone scaffold was confirmed as the key pharmacophoric motif of GA. This scaffold possessed potent inhibitory effect on cancer cell proliferation similar to GA and could serve as a new skeleton of IKKβ inhibitor. We also investigated the binding pattern of this scaffold with IKKβ through molecular docking. The resulted information would help us design more potent derivatives based on this scaffold.

This is the first report to identify 4-oxa-tricyclo[4.3.1.$0^{3,7}$]dec-2-one xanthone scaffold as a new skeleton of IKKβ inhibitor. Our results provided the molecular basis for the antiproliferative effects of GA and its derivatives. Further preclinical and clinical trials are required to determine the anti-tumor efficacy of these compounds.

4. Experimental protocols

4.1. General materials and methods

All reagents were purchased from commercial sources and were used without further purification unless otherwise noted. Melting points were determined by XT-4 melting point apparatus and were reported without any correction. IR spectra were recorded on a Nicolet Impact 410 spectrometer using KBr film. The ^{1}H NMR and ^{13}C NMR spectra were collected on Bruker AV-300 instruments using deuterated solvents with tetramethylsilane (TMS) as internal standard. EI-MS was recorded on Shimadzu GCMS-2010 apparatus. Each of the target compounds were purified by silica gel (60 Å, 70–230 mesh) column chromatography. Concentration and evaporation of the solvent after reaction or extraction was carried out on a rotary evaporator (Büchi Rotavapor) operated at reduced pressure.

GA was isolated and purified according to the previously reported methods [34]. The purity of GA used in all experiments was 95% or higher. It was dissolved in PBS containing arginine to a concentration of 10 mM as the primary stock solution and stored at −20 °C. 3-(4,5-dimethylthiazol-2-yl)-2,5-diphenyltetrazol-ium-bromide (MTT) was purchased from Sigma (St. Louis, MO). Annexin V-FITC Apoptosis Detection kit was purchased from BioVision (Mountain View, CA). Cellomics NF-κB Activation HCS Reagent Kit was obtained from Thermo Scientific (Pittsburgh, PA). HTScan IKKβ kinase assay kit was purchased from Cell Signaling Technology (Beverly, MA). Human IκBα and p-IκBα (ser 32/36) antibodies were

Fig. 5. **20** induced apoptosis in U251 cells. (A) The morphology of U251 cells after exposure to different doses of **20** and GA for 24 h was examined and photographed by an inverted light microscope (200 ×). The cell damage appeared after treatment with **20**, comparing with the control plate (GA). (B) Fluorescence microscope detection of **20** (400 ×). (C) Annexin V/PI double-staining assay of U251 cells. *Y* axis showed PI labeled population and *X* axis shows FITC-labeled Annexin V positive cells. (D) The apoptotic rates of U251 cells induced by **20** and GA. (For interpretation of the references to color in this figure legend, the reader is referred to the web version of this article.)

bought from Santa Cruz Biotechnology, Inc. (Santa Cruz, CA). Histone antibody was bought from Bioworld Technology, Inc. (Bioworld, MN). All drugs were diluted in the corresponding culture medium to desired concentrations before use.

Human U251 glioma cell lines and A549 lung epithelial cell lines were purchased from Cell Bank of Shanghai Institute of Biochemistry and Cell Biology, Shanghai Institutes for Biological Sciences, Chinese Academy of Sciences. U251 and A549 cells were cultured in DMEM which were supplemented with 10% (v/v) fetal calf serum, 100 U/mL penicillin and 100 U/mL streptomycin in a 5% CO_2 atmosphere.

4.2. Chemistry

4.2.1. 1-Hydroxy-3,5,6-tris(2-methylbut-3-yn-2-yloxy)-9H-xanthen-9-one (**2**)

To a solution of **1** (2.9 g, 10.8 mmol) in acetone (100.0 mL), potassium iodide (5.9 g, 35.7 mmol), potassium carbonate (4.9 g, 35.7 mmol) and CuI (0.2 g, 1.1 mmol) were added. The reaction mixture was stirred at room temperature for 10 min, then 2-chloro-2-methylbut-3-*yne* (9.7 mL, 86.4 mmol) was added and the resulted mixture was stirred at 50 °C for 5 h. Water (100.0 mL) and EtOAc (50.0 mL) were added to the mixture and stirred for 30 min. The organic layer was separated, dried over sodium sulfate, and evaporated. The residue was purified through column chromatography (eluent, PE/EtOAc = 8:1) to afford 1.2 g **2** as yellow oil. Yield: 25%. ^{1}H NMR(300 MHz, $CDCl_3$): δ 1.76 (s, 6H), 1.78 (s, 6H), 1.82 (s, 6H), 2.34 (s, 1H), 2.68 (s, 1H), 2.70 (s, 1H), 6.72 (d, J = 2.2 Hz, 1H), 6.82 (d, J = 2.2 Hz, 1H), 7.64 (d, J = 9.0 Hz, 1H), 7.97 (d, J = 9.0 Hz), 12.85 (s, 1H); m/z (EI–MS): 458 $[M]^+$.

4.2.2. 1-Hydroxy-3,5,6-tris(2-methylbut-3-en-2-yloxy)-9H-xanthen-9-one (**3**)

To a solution of **2** (100 mg, 0.2 mmol) in ethanol (10.0 mL) and ethyl acetate (3.3 mL) was added 10% Pd/$BaSO_4$ (10.0 mg). The mixture was stirred under an atmosphere of hydrogen for 2 h at room temperature and filtered through a plug of silica gel. The filtration was concentrated and purified through column chromatography (eluent, PE/EtOAc = 8:1) to afford 81.0 mg **3** as brown oil. Yield: 80%. ^{1}H NMR (300 MHz, $CDCl_3$): 1.55 (s, 6H), 1.60 (s, 6H), 1.66 (s, 6H), 5.17–5.20 (m, 3H), 5.41–5.46 (m, 3H), 5.63–5.70 (m, 3H), 6.42 (d, J = 2.1 Hz, 1H), 6.51 (d, J = 2.1 Hz, 1H), 6.92 (d, J = 10.8 Hz, 1H), 7.35 (d, J = 10.8 Hz, 1H), 12.78 (s, 1H); m/z (EI–MS): 464 $[M]^+$.

4.2.3. Caged xanthone (**4**) and (**5**)

A solution of **3** (100.0 mg, 0.2 mmol) in DMF (3.0 mL) was heated at 120 °C for 1 h. The yellow reaction mixture was cooled to 25 °C and purified by column chromatography (eluent, PE/EtOAc = 5:1) to yield the caged xanthone **4** (50.0 mg, Yield: 50%) and **5** (15.0 mg, Yield: 15%).

4: yellow solid; m.p. > 200 °C ^{1}H NMR (300 MHz, $CDCl_3$): δ 1.04 (s, 3H), 1.24–1.26 (m, 4H), 1.38 (s, 3H), 1.69 (s, 3H), 1.76 (s, 3H), 1.81 (s, 3H), 2.35 (dd, J = 13.2 Hz, J = 4.4 Hz, 1H), 2.46 (d, J = 9.2 Hz, 1H), 2.56–2.59 (m, 2H), 3.41–3.49 (m, 2H), 3.50–3.53 (m, 1H), 4.30–4.45 (m, 1H), 5.22–5.27 (m, 1H), 6.04 (s, 1H), 6.09 (br s, 1H), 7.46 (d, J = 6.8 Hz, 1H), 12.60 (s, 1H); ^{13}C NMR ($CDCl_3$, 75 MHz) δ 16.9, 18.2, 22.3, 25.6, 25.7, 25.9, 29.0, 29.2, 30.3, 47.0, 49.2, 83.2, 84.5, 90.5, 97.0, 101.0, 105.6, 117.7, 121.1, 133.3, 133.9, 134.9, 135.4, 157.9, 163.0, 163.9, 179.4, 203.1; m/z (ESI–MS): 463 $[M-H]^-$; HRMS (ESI–TOF) calcd. for $C_{28}H_{32}O_6$ $[M+Na]^+$ 487.2097, found 487.2104.

5: yellow solid; m.p. > 200 °C ^{1}H NMR (300 MHz, $CDCl_3$): δ 1.12 (s, 3H), 1.30 (s, 3H), 1.36 (dd, J = 13.6 Hz, J = 10.5 Hz, 1H), 1.40 (s, 3H), 1.67 (s, 3H), 1.77 (d, J = 1.1 Hz, 3H), 1.82 (s, 3H), 2.33 (dd, J = 13.6 Hz, J = 4.5 Hz, 1H), 2.39 (d, J = 9.6 Hz, 1H), 2.61–2.59 (m, 2H), 3.37 (m, 2H), 3.48 (dd, J = 6.8, J = 4.3 Hz, 1H), 4.48–4.44 (m, 1H), 5.26–5.23 (m, 1H), 6.08 (s, 1H), 6.60 (br s, 1H), 7.40 (d, J = 6.8 Hz, 1H), 12.80 (s, 1H); m/z (ESI–MS): 463 $[M-H]^-$ [35].

4.2.4. 2,3,4-Trisbenzyloxyacetophenone (**7**)

Compound **6** (1.7 g, 10 mmol) was added to the suspension of benzyl bromide (6.0 g, 35.0 mmol), K_2CO_3 (8.0 g, 58.0 mmol) and KI (0.3 g, 1.5 mmol) in DMF (20.0 mL). The reaction mixture was heated to 50 °C for 8 h. Then the reaction mixture was cooled to room temperature and poured into ethyl acetate (100 mL) and washed with brine. The organic layer was dried with Na_2SO_4 followed concentration under reduced pressure. The residue was purified through column chromatography (eluent, PE/EtOAc = 4:1) to afford 3.7 g **7** as light yellow solid. Yield: 85%. m.p.: 71–73 °C ^{1}H NMR (300 MHz, $CDCl_3$): δ 2.30 (s, 3H), 5.02 (s, 2H), 5.08 (s, 2H), 5.14 (s, 2H), 6.62 (d, J = 9.0 Hz, 1H), 7.28–7.33 (m, 6H), 7.34–7.38 (m, 10H); m/z (EI–MS): 438 $[M]^+$.

4.2.5. 2-Hydroxy-3,4-bisbenzyloxyacetophenone (**8**)

To a solution of **7** (2.0 g, 4.6 mmol) in toluene (20.0 mL) was added trifluoroacetic acid (4.0 mL). The dark reaction mixture was stirred at room temperature for 2 h. Then the mixture was neutralized with 10% NaOH aqueous and extracted with ethyl acetate. The organic layer was dried with Na_2SO_4 followed concentration under reduced pressure. The residue was purified through column chromatography (eluent, PE/EtOAc = 4:1) to afford 1.1 g **8** as light yellow solid. Yield: 70%. m.p.: 122–123 °C ^{1}H NMR (300 MHz, $CDCl_3$): δ 2.22 (s, 3H), 5.10 (s, 2H), 5.15 (s, 2H), 6.58 (d, J = 10.2 Hz, 1H), 7.28–7.34 (m, 6H), 7.35–7.40 (m, 5H), 11.12 (s, 1H); m/z (EI–MS): 348 $[M]^+$.

4.2.6. Chalcone compounds (**9a**) and (**9b**)

To a cold solution of **8** (500.0 mg, 1.4 mmol) and appropriate benzaldehyde in 3 mL H_2O/EtOH (1:4, v/v), 3.0 mL 20% KOH solution was added. The resulting mixture was stirred at room temperature for 36 h. The mixture was poured into ice, acidified to pH ~ 5 with 1 N HCl, and extracted with ethyl acetate. The organic phase was washed with brine, dried over anhydrous Na_2SO_4, and concentrated in vacuo. The residue was purified through column chromatography (eluent, PE/EtOAc = 6:1) to afford **9a** or **9b**.

9a, reagent: benzaldehyde (168.5 mg, 1.6 mmol). 388.4 mg; Yield: 62%; yellow solid; m.p.: 164–165 °C ^{1}H NMR (300 MHz, $CDCl_3$): δ 5.10 (s, 2H), 5.17 (s, 2H), 6.47 (d, J = 10.8 Hz, 1H), 7.08 (d, J = 9.6 Hz, 2H), 7.34–7.58 (m, 12H), 7.73 (d, J = 9.6 Hz, 2H), 7.80 (d, J = 10.8 Hz, 1H); 13.03 (s, 1H); m/z (EI–MS): 436 $[M]^+$.

9b, reagent: 4-benzyloxy benzaldehyde (335.0 mg, 1.6 mmol). 529.5 mg; Yield: 68%; yellow solid; m.p.: 161–162 °C ^{1}H NMR (300 MHz, $CDCl_3$): δ 5.12 (s, 2H), 5.14 (s, 2H), 5.18 (s, 2H), 6.52 (d, J = 9.0 Hz, 1H), 7.02 (d, J = 9.0 Hz, 2H), 7.28–7.67 (m, 13H), 7.73 (d, J = 9.0 Hz, 2H), 7.74 (d, J = 9.0 Hz, 1H), 7.86 (d, J = 15.0 Hz, 1H); 13.33 (s, 1H); m/z (EI–MS): 542 $[M]^+$.

4.2.7. Flavone compounds (**10a**) and (**10b**)

A stirred solution of corresponding Flavones **9a** (500.0 mg, 1.1 mmol) or **9b** (600.0 mg, 1.1 mmol) and iodine (28.0 mg, 0.1 mmol) in DMSO (10.0 mL) was heated to 110 °C for 12 h. The mixture was cooled and poured into cold water. The mixture was extracted with ethyl acetate. The combined organic phase was washed with saturated sodium thiosulfate and water, successively. Then the organic layer was dried with anhydrous Na_2SO_4 and concentrated. The residue was purified by silica gel column chromatography (eluent, PE/EtOAc = 6:1) to afford **10a** or **10b**.

10a: 355.0 mg; Yield: 71%; yellow solid; m.p. > 200 °C ^{1}H NMR (300 MHz, $CDCl_3$): δ 5.22 (s, 2H), 5.30 (s, 2H), 6.91 (s, 1H), 7.15 (d, J = 9.0 Hz, 1H), 7.31–7.40 (m, 3H), 7.42–7.53 (m, 11H), 7.75 (d, J = 8.4 Hz, 2H), 7.90 (d, J = 9.0 Hz, 2H) m/z (EI–MS): 434 $[M]^+$.

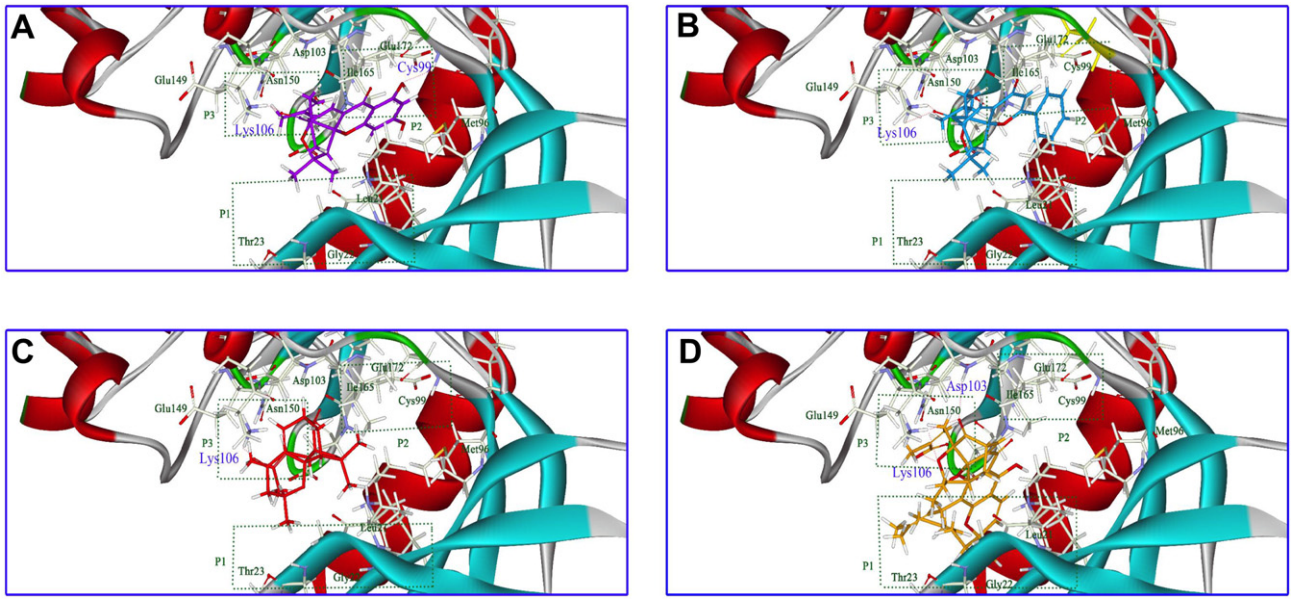

Fig. 7. Molecular docking simulations for GA and its derivatives with IKKβ. (A) Compound **20**; (B) Compound **14**; (C) Compound **21**; (D) GA. Residues in the binding pocket were shown as gray stick. H-bonds were shown as red dot line. (For interpretation of the references to colour in this figure legend, the reader is referred to the web version of this article.)

10b: 410.0 mg; Yield: 69%; yellow solid; m.p. > 200 °C ^{1}H NMR (300 MHz, $CDCl_3$): δ 5.20 (s, 2H), 5.24 (s, 2H), 5.35 (s, 2H), 6.84 (s, 1H), 7.15 (d, J = 8.4 Hz, 2H), 7.31–7.52 (m, 16H), 7.75 (d, J = 8.1 Hz, 1H), 7.90 (d, J = 8.4 Hz, 2H) m/z (EI–MS): 540 $[M]^+$.

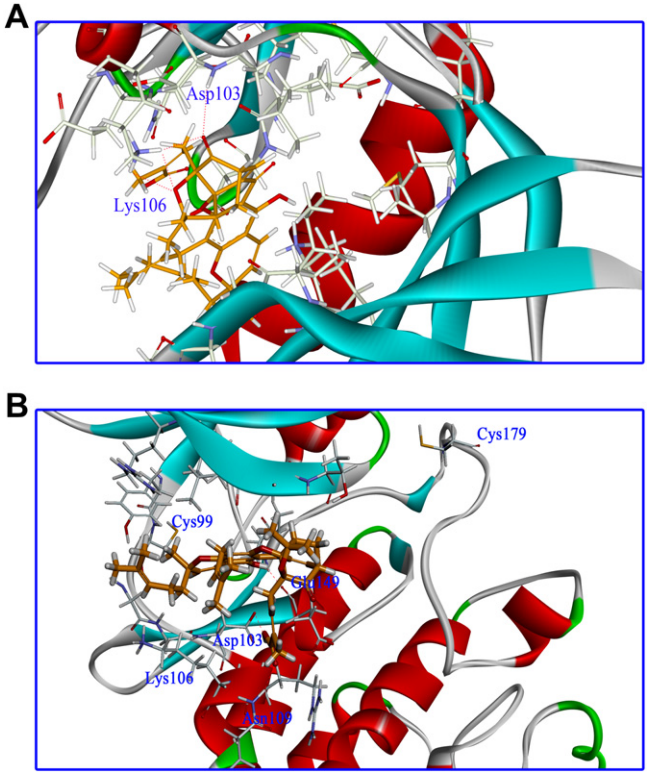

Fig. 8. The binding pattern comparison of GA with IKKβ. (A) GA with the homology model of IKKβ. (B) GA with the crystal structure of IKKβ. Residues in the binding pocket were shown as gray stick. H-bonds were shown as red dot line. (For interpretation of the references to colour in this figure legend, the reader is referred to the web version of this article.)

*4.2.8. Flavone compounds (**11a**) and (**11b**)*

To a solution of compound **10a** (4.3 g, 10.0 mmol) or **10b** (5.4 g, 10.0 mmol) in THF/CH_3OH (40.0 mL/40.0 mL) was added 10% Pd/C (0.5 g). The reaction mixture was stirred under an atmosphere of hydrogen overnight. The reaction mixture was filtered and concentrated under reduced pressure. The residue was purified by silica gel column chromatography (eluent, PE/EtOAc = 6:1) to afford **11a** or **11b**.

11a: 2.1 g; Yield: 83%; yellow solid; m.p. > 200 °C ^{1}H NMR (300 MHz, $CDCl_3$): δ 6.90 (s, 1H), 6.96 (d, J = 8.4 Hz, 1H), 7.41 (d, J = 8.4 Hz, 1H), 7.58–7.60 (m, 3H), 8.14–8.17 (m, 2H), 9.50 (s, 1H), 10.35 (s, 1H). m/z (EI–MS): 254 $[M]^+$.

11b: 2.2 g; Yield: 81%; yellow solid; m.p. > 200 °C ^{1}H NMR (300 MHz, $CDCl_3$): δ 6.70 (s, 1H), 6.92 (d, J = 7.8 Hz, 2H), 7.37 (d, J = 8.4 Hz, 2H), 8.00 (d, J = 8.4 Hz, 2H), 9.40 (s, 1H), 10.21 (s, 2H). m/z (EI–MS): 270 $[M]^+$.

*4.2.9. Flavone compounds (**12a**) and (**12b**)*

To a solution of **11a** (500.0 mg, 2.1 mmol) or **11b** (555.0 mg, 2.1 mmol) in acetone (20.0 mL), potassium iodide (1.7 g, 10.5 mmol), potassium carbonate (1.5 g, 10.5 mmol) and CuI (114.6 mg, 0.6 mmol) were added. The reaction mixture was stirred at room temperature for 10 min, then 2-chloro-2-methylbut-3-yne (1.72 g, 16.8 mmol) was added and the resulted mixture was stirred at 50 °C for 4 h. Water (30.0 mL) and EtOAc (30.0 mL) were added to the mixture and stirred for 30 min. The organic layer was separated, dried over sodium sulfate, and evaporated. The residue was purified through column chromatography (eluent, PE/EtOAc = 8:1) to afford **12a** or **12b**.

12a: 470.1 mg; Yield: 62%; white solid; m.p.: 163–165 °C ^{1}H NMR (300 MHz, $CDCl_3$): δ 1.74 (s, 6H), 1.83 (s, 6H), 2.29 (s, 1H), 2.65 (s, 1H), 6.74 (s, 1H), 7.49 (m, 3H), 7.66 (d, J = 8.7 Hz, 1H), 7.92 (d, J = 8.7 Hz, 1H), 8.02 (m, 2H). m/z (EI–MS): 386 $[M]^+$.

12b: 577.2 mg; Yield: 60%; white solid; m.p.: 152–153 °C ^{1}H NMR (300 MHz, $CDCl_3$): δ 1.68 (s, 6H), 1.73 (s, 6H), 1.86 (s, 6H), 2.29 (s, 1H), 2.51 (s, 1H), 2.65 (s, 1H), 6.72 (s, 1H), 6.80 (d, J = 10.5 Hz, 1H), 7.05 (d, J = 11.7 Hz, 2H), 7.49 (d, J = 10.5 Hz, 1H), 7.82 (d, J = 11.7 Hz, 2H). m/z (EI–MS): 468 $[M]^+$.

*4.2.10. Flavone compounds (**13a**) and (**13b**)*

To a solution of **12a** (200.0 mg, 0.5 mmol) or **12b** (242.4 mg, 0.5 mmol) in ethanol (10.0 mL) and ethyl acetate (3.3 mL) was added 10% $Pd/BaSO_4$ (20.0 mg). The mixture was stirred under an atmosphere of hydrogen for 2 h at room temperature and filtered through a plug of silica gel, the filtration was concentrated and purified through column chromatography (eluent, PE/EtOAc = 8:1) to afford **13a** or **13b**.

13a: 155.6 mg; Yield: 77%; light yellow oil. ^{1}H NMR (300 MHz, $CDCl_3$): δ 1.54 (s, 6H), 1.58 (s, 6H), 4.88 (dd, J = 10.8 Hz, J = 1.8 Hz, 1H), 5.10–5.22 (m, 3H), 6.34 (m, 2H), 6.66 (s, 1H), 7.10 (d, J = 9.0 Hz, 1H), 7.42 (m, 3H), 7.73 (dd, J = 9.0 Hz, J = 0.9 Hz, 1H), 7.86 (m, 2H); m/z (EI–MS): 390 $[M]^+$.

13b: 198.5 mg; Yield: 81%; light yellow oil. ^{1}H NMR (300 MHz, $CDCl_3$): δ 1.53–1.56 (m, 18H), 4.99 (d, J = 10.8 Hz, 1H), 5.12–5.29 (m, 5H), 6.11–6.31 (m, 3H), 6.67 (s, 1H), 7.10 (d, J = 9.0 Hz, 2H), 7.15 (d, J = 9.0 Hz, 1H), 7.80 (d, J = 9.0 Hz, 1H), 7.85 (d, J = 9.0 Hz, 2H); m/z (EI–MS): 474 $[M]^+$.

*4.2.11. Caged flavones (**14**) and (**15**)*

To a solution of **13a** (100.0 mg, 0.3 mmol) or **13b** (100.0 mg, 0.2 mmol) in DMF (3.0 mL) was heated at 120 °C for 1 h. The yellow reaction mixture was cooled to 25 °C and the mixture was purified by column chromatography (eluent, PE/EtOAc = 4:1) to yield the caged flavone **14** or **15**.

14: 51.0 mg; Yield: 51%; white solid; m.p.: 146–148 °C ^{1}H NMR (300 MHz, $CDCl_3$): δ 1.32 (s, 6H), 1.38 (m, 1H), 1.42 (s, 3H), 1.71 (s, 3H), 2.35 (dd, J = 13.3, J = 4.5, 1H), 2.53 (d, J = 9.5 Hz, 1H), 2.57–2.66 (m, 2H), 3.48 (dd, J = 7.0, J = 4.5, 1H), 4.69 (m, 1H), 6.13 (s, 1H), 7.30 (d, J = 7.0, 1H), 7.57–7.46 (m, 3H), 7.85–7.82 (m, 2H); ^{13}C NMR (75 MHz, $CDCl_3$): δ 17.9, 25.2, 25.8, 29.3, 29.4, 30.5, 46.6, 49.7, 83.6, 84.3, 92.6, 100.9, 117.8, 126.6, 128.9, 131.0, 131.8, 132.8, 134.2, 134.6, 168.5, 177.2, 203.1; m/z (ESI–MS): 389 $[M - H]^-$; HRMS (ESI–TOF) calcd. for $C_{25}H_{27}O_4$ $[M + H]^+$ 391.1909, found 391.1914.

15: 44.5 mg; Yield: 45%; light yellow solid; 152–154 °C ^{1}H NMR (300 MHz, $CDCl_3$): δ 1.31 (s, 6H), 1.37 (s, 3H), 1.68–1.77 (m, 9H), 1.71 (s, 3H), 2.34 (dd, J = 13.2, J = 4.2, 1H), 2.54 (d, J = 9.6, 1H), 2.58–2.67 (m, 2H), 3.44 (d, J = 7.8, 2H), 3.47 (dd, J = 7.0, J = 4.2 Hz, 1H), 4.70 (m, 1H), 5.33 (m, 1H), 6.06 (s, 1H), 6.37 (br-s, 1H),6.92 (d, J = 7.8, 1H), 7.30 (s, 1H), 7.59–7.62 (m, 2H); ^{13}C NMR (75 MHz, $CDCl_3$): δ 8.85, 21.24, 25.86, 29.07, 29.10, 30.12, 48.80, 48.95, 63.16, 83.47, 84.36, 91.05, 101.90, 106.87, 134.81, 135.76, 139.75, 150.23, 153.68, 162.07, 164.57, 170.08, 175.43, 197.08, 203.93; m/z (ESI–MS): 473 $[M - H]^-$; HRMS (ESI–TOF) calcd. for $C_{25}H_{27}O_4$ $[M + H]^+$ 475.2484, found 475.2496.

*4.2.12. 1,3-Bishydroxy-9H-xanthen-9-one (**16**)*

To a round-bottomed flask containing phloroglucinol (10.0 g, 79.3 mmol), salicylic acid (10.9 g, 79.3 mmol) and $ZnCl_2$ (70.0 g, 515.0 mmol) was added $POCl_3$ (120.0 mL). The reaction mixture was stirred for 3.5 h at 70 °C under N_2. It was then cooled to 25 °C and poured into a beaker of ice. The reaction mixture was filtered and the filter cake was washed with saturated NaCl to get the crude material which was purified by silica gel column chromatography (eluent, PE/EtOAc = 4:1) to afford 7.8 g **16** as yellow solid. Yield: 43%; m.p.>200 °C; ^{1}H NMR (300 MHz, $CDCl_3$): δ 6.22 (d, J = 1.8, 1H), 6.41 (d, J = 1.8, 1H), 7.47 (t, J = 7.5 Hz, 1H), 7.60 (d, J = 8.4 Hz, 1H), 7.86 (t, J = 7.5 Hz, 1H), 8.13 (d, J = 8.4 Hz, 1H), 11.14 (br-s, 1H), 12.83 (s, 1H); m/z (EI–MS): 228 $[M]^+$.

*4.2.13. 1,3-Dihydroxy-4-(3-methylbut-2-enyl)-9H-xanthen-9-one (**17**)*

To a solution of **16** (2.0 g, 8.8 mmol) in methanol (70.0 mL), sodium methoxide (2.5 g, 43.9 mmol) was added slowly and then stirred for 15 min. 1-bromo-3-methyl-2-butene (2.0 g, 13.2 mmol) was added dropwise at 0 °C and the resulted mixture was stirred at room temperature for 12 h. After adding 50 mL dichloromethane, the mixture was neutralized with 2N HCl. The organic layer was separated, dried over sodium sulfate, and evaporated. The residue was purified through column chromatography (eluent, PE/EtOAc = 16:1) to afford 277.0 mg **17** as light yellow solid. Yield: 11%; m.p.: 172–174 °C; ^{1}H NMR (300 MHz, $CDCl_3$): δ 1.72 (s, 3H), 1.15–1.30 (m, 7H), 1.86 (s, 3H), 3.59 (d, J = 7.2 Hz, 2H), 5.30 (t, J = 7.2 Hz, 1H), 6.15 (s, 1H), 6.31 (s, 1H), 7.38 (dd, J = 7.8 Hz, J = 1.5 Hz, 1H), 7.46 (d, J = 8.4 Hz, 1H), 7.70 (dd, J = 7.8 Hz, J = 1.5 Hz, 1H), 8.26 (d, J = 1.5 Hz, 1H), 12.91 (s, 1H); m/z (EI–MS): 296 $[M]^+$.

*4.2.14. Caged xanthone (**18**)*

The synthesis method of **18** was reported previously by our group [24]. **18**: yellow solid; m.p.: 124–126 °C ^{1}H NMR (300 MHz, $CDCl_3$) δ 0.84 (s, 3H), 1.15–1.30 (m, 7H), 1.66 (s, 3H), 2.27 (dd, J = 13.5 Hz, J = 4.5 Hz, 1H), 2.39 (d, J = 9.6 Hz, 1H), 2.55 (d, J = 9.3 Hz, 2H), 3.41–3.47 (m, 1H), 4.35 (t, 1H), 6.97–7.02 (m, 2H), 7.36 (d, J = 6.9 Hz, 1H), 7.45 (dd, J = 8.4 Hz, J = 7.2 Hz, 1H), 7.87 (d, J = 8.4 Hz, 1H); ^{13}C NMR (CDCl3): 16.69, 25.14, 25.33, 29.12, 30.33, 30.93, 46.84, 48.83, 83.52, 84.62, 90.37, 118.10, 118.97, 119.14, 121.87, 126.99, 133.76, 134.78, 134.94, 136.21, 159.67, 176.52, 203.02. m/z (ESI–MS): 363 $[M - H]^-$; HRMS (ESI–TOF) calc. for $C_{23}H_{24}O_4$ $[M + H]^+$ 365.1753, found 365.1766.

*4.2.15. Caged xanthone (**19**)*

Compound **19** was synthesized in our laboratory [24]. **19**: yellow solid; m.p.: 130–132 °C ^{1}H NMR (300 MHz, $CDCl_3$): δ 0.95 (s, 3H), 1.18–1.25 (m, 4H), 1.30 (s, 3H), 1.61 (s, 3H), 2.26 (dd, J = 13.5 Hz, J = 4.5 Hz, 1H), 2.37 (d, J = 9.6 Hz, 1H), 2.54 (d, J = 7.8 Hz, 2H), 3.44 (dd, J = 6.9 Hz, J = 4.5 Hz, 1H), 4.34 (m, 1H), 6.43 (dd, J = 8.1 Hz, J = 0.9 Hz, 1H), 6.45 (dd, J = 8.1 Hz, J = 0.9 Hz, 1H), 7.32 (t, J = 8.1 Hz, 1H), 7.41 (d, J = 9.6 Hz, 1H), 12.00 (s, 1H). ^{13}C NMR ($CDCl_3$): δ 16.68, 24.95, 25.49, 29.05, 29.14, 30.27, 46.98, 48.82, 83.53, 84.46, 90.02, 106.12, 107.38, 109.37, 118.64, 133.88, 134.90, 135.30, 138.75, 159.59, 162.90, 181.33, 202.69. m/z (ESI–MS): 379 $[M - H]^-$; HRMS (ESI–TOF) calc. for $C_{23}H_{24}O_6$ $[M + Na]^+$ 403.4337, found 403.4342.

*4.2.16. Caged chromanone (**21**)*

Compound **21** was synthesized using method reported by our laboratory [24]. **21**: yellow solid; m.p.: 155–156 °C ^{1}H NMR (CDCl3): 1.18 (s, 3H), 1.24–1.36 (m, 4H), 1.42 (s, 3H), 1.51 (s, 3H), 1.54 (s, 3H), 2.09 (dd, J = 18 Hz, J = 16 Hz, 1H), 2.23–2.41 (m, 3H), 2.52–2.66 (m, 2H), 3.23–3.30 (m,1H), 4.0–4.07 (m, 1H), 4.33 (m, 1H), 7.17 (d, J = 7.2 Hz, 1H); ^{13}C NMR (CDCl3): 17.55, 20.66, 25.05, 27.39, 28.38, 28.42, 29.76, 44.4, 44.77, 45.74, 66.08, 82.37, 83.88, 86.58, 118.99, 133.06, 134.48, 136.18, 191.96, 203.33. m/z (ESI): 353 $[M + Na]^+$. Anal. Calcd for $C_{20}H_{26}O_4$ (%): C,72.70; H, 7.93; Found: C, 72.87; H, 7.93.

*4.2.17. 7,9-Dihydroxy-2,2-diphenyl-6H-[1,3]dioxolo[4,5-c]xanthen-6-one (**22**)*

Compound **1** (0.13 g, 0.5 mmol) was added to diphenyl ether (10 mL) and then dichlorodiphenylmethane (0.18 g, 0.75 mmol) was added. The reaction mixture was heated to 175 °C for 0.5 h under N_2. The reaction mixture cooled to room temperature was poured into petroleum ether (100 mL). The precipitate was collected by filtration and washed with petroleum ether, which was purified by silica gel column chromatography (petroleum ether/EA 8:1). Compound **22** (0.18 g, 85%) was obtained : light yellow solid; m.p.: 212–214 °C; ^{1}H NMR (300 MHz, CD_3COCD_3): δ 6.26 (d, J = 2.2 Hz, 1H), 6.46 (d, J = 2.2 Hz, 1H), 7.13 (d, J = 8.5 Hz, 1H), 7.48 (m, 6H), 7.66 (m, 4H), 7.82 (d, J = 8.5 Hz, 1H), 9.83 (s, 1H), 12.99 (s, 1H); EI–MS (m/z) 424 $(M)^+$.

4.2.18. 7-Hydroxy-9-(methoxymethoxy)-2,2-diphenyl-6H-[1,3] dioxolo[4,5-c]xanthen-6-one (**23**)

At room temperature K_2CO_3 (1.1 g, 8 mmol) was added to the solution of compound **22** (1.70 g, 4 mmol) in acetone (50 mL). After stirred for 15 min, to this mixture was added MOMCl (0.46 mL, 6 mmol). The reaction mixture was stirred for 6 h and poured into H_2O (150 mL). The precipitate was collected by filtration and washed with water, which was purified by silica gel column chromatography (petroleum ether/EtOAc 8:1) to give the compound **23** (1.68 g, 90%) as a white solid: m.p: 125–127 °C; ^{1}H NMR (300 MHz, $CDCl_3$): δ 3.50 (s, 3H), 5.24 (s, 2H), 6.45 (d, J = 2.2 Hz, 1H), 6.65 (d, J = 2.2 Hz, 1H), 6.97 (d, J = 8.5 Hz, 1H), 7.40 (m, 6H), 7.64 (m, 4H), 7.87 (d, J = 8.5 Hz, 1H), 12.89 (s, 1H); EI–MS(m/z): 468 $(M)^+$.

4.2.19. 9-(methoxymethoxy)-6-oxo-2,2-diphenyl-6H-[1,3]dioxolo [4,5-c]xanthen-7-yl acetate (**24**)

Ac_2O (1.7 g, 16.7 mmol) was added to a solution of compound **23** (6.0 g, 12.8 mmol) and DMAP (2.35 g, 0.193 mmol) in dichlormethane (100 mL). The reaction mixture was stirred for 0.5 h at room temperature. Another dichlormethane (100 mL) was added to dilute and the reaction mixture was washed with H_2O (100 mL*3). The organic layer was dried with Na_2SO_4 and concentrated under reduce pressure. The residue was purified by silica gel column chromatography (petroleum ether/EtOAc 4:1) to give the compound **24** (5.9 g, 91%) as a white solid: m.p: 192–193 °C; ^{1}H NMR (300 MHz, $CDCl_3$): δ 2.46 (s,3H), 3.51 (s, 3H), 5.27 (s, 2H), 6.67 (d, J = 2.1 Hz, 1H), 6.94 (d, J = 8.4 Hz, 1H), 7.09(d, J = 2.1 Hz, 1H), 7.26 (m, 6H), 7.41 (m, 4H), 7.87 (d, J = 8.4 Hz, 1H); EI–MS(m/z): 510 $(M)^+$.

4.2.20. 5,6-Dihydroxy-3-(methoxymethoxy)-9-oxo-9H-xanthen-1-yl acetate (**25**)

To a solution of compound **24** (5.9 g, 11.6 mmol) in THF/MeOH (40 mL/40 mL) was added 10% Pd/C (0.59 g). The reaction mixture was stirred at 50 °C under an atmosphere of hydrogen overnight. The reaction mixture was filtered and concentrated under reduce pressure. The residue was pulped with petroleum ether/EtOAc (50 mL/10 mL) and filtered to give the compound **25** (3.6 g, 90%) as white solid: m.p: 149–151 °C; ^{1}H NMR (300 MHz, $CDCl_3$): δ 2.50 (s, 3H), 3.51 (s, 3H), 5.22 (s, 2H), 6.65 (d, J = 2.4 Hz, 1H), 6.86 (d, J = 9 Hz, 1H), 6.94 (d, J = 2.4 Hz, 1H) 7.64 (d, J = 9 Hz, 1H); EI–MS(m/z): 346 $(M)^+$.

4.2.21. 3-(methoxymethoxy)-5,6-bis(2-methylbut-3-yn-2-yloxy)-9-oxo-9H-xanthen-1-yl acetate (**26**)

To a solution of xanthone **25** (0.55 g, 1.6 mmol) in dried acetone (5 mL) was added KI (0.79 g, 4.8 mmol), K_2CO_3 (0.66 g, 4.8 mmol), CuI (0.03 g, 0.16 mmol) and 2-chloro-2-methylbut-3-yne (1.6 g, 16 mmol). The reaction mixture was heated at reflux for 1.5 h under nitrogen. It was then cooled to 25 °C and filtered. The filtration was concentrated and the residue was purified by silica gel column chromatography (petroleum ether/EtOAc 8:1) to give the compound **26** (0.56 g, 70%) as a light yellow solid: m.p: 133–136 °C; ^{1}H NMR (300 MHz, $CDCl_3$): δ 1.75 (s,6H), 1.80 (s,6H), 2.34(s,1H), 2.48(s, 3H), 2.64 (s, 1H), 3.51 (s, 3H), 5.26 (s, 2H), 6.69 (d, J = 2.1 Hz, 1H), 7.03 (d, J = 2.1 Hz, 1H), 7.57 (d, J = 9 Hz, 1H), 7.93 (d, J = 9 Hz, 1H); ESI–MS(m/z): 479M + H^+.

4.2.22. Caged xanthone (**27**)

To a solution of xanthone **26** (0.22 g, 0.46 mmol) in alcohol (10 mL) was added 10% Pd/$BaSO_4$ (22 mg). The reaction mixture was degassed using hydrogen and stirred under an atmosphere of hydrogen for 0.5 h at room temperature. The reaction mixture was filtered and concentrated under reduce pressure. The residue need not be purified and dissolved in DMF (5 mL). The solution was heated at 120 °C for 1 h under N_2. DMF was removed under reduce pressure and the residue was purified by silica gel column chromatography (petroleum ether/EtOAc 8:1) to give the compound **27** (0.14 g, 65%) as a yellow solid: m.p: 169–171 °C; ^{1}H NMR (300 MHz, $CDCl_3$): δ 1.41 (s, 3H), 1.31 (s, 3H), 1.35 (d, 1H, J = 9.9 Hz), 1.53 (s, 3H), 1.69 (s, 3H), 2.30 (dd, 1H, J = 13.5 Hz, J = 4.5 Hz), 2.38 (s, 3H), 2.42 (d, 1H, J = 9.6 Hz), 2.60 (d, 2H, J = 8.1 Hz), 3.49 (m, 4H), 4.47–4.48 (m, 1H), 5.22 (s, 2H), 6.41 (d, 1H,J = 2.4 Hz), 6.58 (d, 1H, J = 2.4 Hz), 7.30 (d, 1H, J = 6.9 Hz); ^{13}C NMR (CDCl3, 75 MHz) δ 17.0, 21.1, 25.4, 29.0, 30.4, 46.8, 48.7, 56.6, 83.3, 84.4, 90.5, 94.2, 102.1, 106.3, 107.3, 118.3, 133.1, 135.1, 135.1, 152.3, 162.1, 163.2, 169.4, 173.9, 203.1; m/z (EI): 505M + Na^+, 483M + H^+; HRMS(ESI–TOF) found 505.1834 (calcd for C27H30O8+Na^+ 505.1838).

4.2.23. Caged xanthone (**20**)

To a solution of xanthone **27** (0.48 g, 1.0 mmol) in acetone (3.0 mL) was added 3M HCl (1.0 mL). The reaction mixture was stirred under 40 °C for 6 h at room temperature. The reaction mixture was concentrated under reduce pressure. The residue was purified by silica gel column chromatography (petroleum ether/EtOAc 6:1) to give the compound **20** (0.24 g, 60%): yellow solid; m.p: 168–170 °C ^{1}H NMR (300 MHz, $CDCl_3$): δ 1.11 (s, 3H), 1.23 (s, 3H), 1.33 (s, 3H), 1.61 (s, 3H), 2.26 (dd, J = 13.5 Hz, J = 4.5 Hz, 1H), 2.37 (d, J = 9.6 Hz, 1H), 2.54 (d, J = 7.8 Hz, 2H), 3.44 (m, 2H), 4.37 (m, 1H), 5.96 (d, J = 2.1 Hz, 1H), 5.98 (d, J = 2.1 Hz, 1H), 7.35 (d, J = 6.9 Hz, 1H), 12.40 (s, 1H); ^{13}C NMR ($CDCl_3$): δ 16.80, 26.20, 26.60, 30.06, 30.14, 32.22, 48.68, 49.94, 84.63, 85.46, 91.13, 107.14, 108.34, 109.40, 120.64, 135.84, 136.95, 137.30, 140.75, 159.52, 165.61, 182.36, 206.60. m/z (ESI–MS): 395 $[M - H]^-$; HRMS (ESI–TOF) calc. for $C_{23}H_{24}O_6$ $[M + Na]^+$ 419.1471, found 419.1478.

4.3. Assays for cell viability, apoptosis, and cell cycle distribution

Cells viabilities were measured by a colorimetric assay using MTT as described previously [37]. Vitality Index (%) was calculated using the following equation: $Vitality\ Index(\%) = (A_{treatment}/A_{control}) \times 100\%$. Apoptotic cells were assayed according to the method described previously [36,38]. Apoptotic or necrotic cells were identified by dual staining with recombinant fluorescein isothiocyanate (FITC)-conjugated with Annexin V and propidium iodide (PI) (Sigma, St. Louis, MO). The experiment was performed according to manufacturer's instructions (Becton Dickinson, Franklin Lakes, NJ). For cell cycle distribution assay, cells were trypsinized, washed with PBS, and fixed in 1.5 mL 95% ethanol at 4 °C overnight followed by incubation with RNase and staining by propidium iodide (PI). Data acquisition was performed with a Becton Dickinson FACS Calibur flow cytometer (Franklin Lakes, NJ).

4.4. NF-κB translocation detection using high-content screening

The NF-κB translocation experiment was performed according to Thermo's instructions. Briefly, A549 cells were plated into 96-well plates at 9000 cells per well and then serum-starved for 18 h. Different concentrations of GA was added and the plate was incubated at 37 °C for 2 h. Mixed stimulators containing TNFα (50 ng/mL), IFN-γ (100 U/mL) and IL-1β (100 U/mL) were added and the plate was incubated at 37 °C for 30 min. Culture medium was aspirated and 100 μl of pre-warmed fixation solution was added to each well. After incubation at room temperature for 15 min, fixation solution was aspirated and the plate was washed twice. 100 μl of 1 × permeabilization buffer was then added and incubated for 15 min. Permeabilization buffer was aspirated and washed twice. 50 μl of primary antibody solution was then added and incubated for 1 h, followed by two washes. 100 μl of blocking buffer was then added, and after 15 min incubation, 50 μl of secondary antibody solution was added and incubated for 45 min protected from light.

After another two washes, the plate was sealed and evaluated on KineticScan HCS Reader (Thermo Scientific, Pittsburgh, PA).

4.5. Preparation of cytoplasmic and nuclear extracts

To determine the effect of GA on TNF-dependent p65 translocation, cytoplasmic or nuclear extracts were prepared as described previously [40]. To reduce the constitutive signal for NF-κB activation, exponentially growing U251 cells were serum-starved overnight and then preincubated with GA for 4 h before being stimulated with TNFα for 30 min. Cells were washed once with ice-cold PBS and scraped into 1 ml of PBS. Cells were centrifuged at 14,000 g/min and resuspended in 200 μl buffer A, which was composed of (in mM) 10 HEPES, pH 7.9, 10 KCl, 0.1 EDTA, 0.2 EGTA, 1 DTT, and 0.5 PMSF for 15 min, before 13 μl of 10% Nonidet P-40 was added. Cells were then vortexed for 10 s before being centrifuged again at 14,000 g/min for 30 s. The cytoplasmic supernatant was removed, and the nuclear pellet was resuspended in 30 μl of buffer C (20 mM HEPES, pH 7.9, 0.4 M NaCl, 1 mM EDTA, 1 mM EGTA, 25% glycerol, 1 mM DTT, and 1 mM PMSF) and shaken for 15 min before being centrifuged for 5 min at 14,000 g/min. The supernatant was retained, and the protein concentration was determined by the BCA assay method with Varioskan spectrofluorometer and spectrophotometer (Thermo, Waltham, MA) at 562 nm. Samples were stored at −80 °C until use.

4.6. Flow cytometry

Annexin V-FITC apoptosis detection kit (BioVision, Mountain View, CA) assay was performed according to the manufacturer's protocol. Briefly, cells were treated with compound **20** (4, 8 and 16 μM) and GA (8 μM) for 24 h and washed with PBS. Then the cells were collected, resuspended in binding buffer (pH 7.5, 10 mM HEPES, 2.5 mM $CaCl_2$ and 140 mM NaCl), and incubated with Annexin V-FITC and then PI for 10 min in the dark at room temperature. Cells were then analyzed by flow cytometry (FACS Calibur, Becton Dickinson, Franklin Lakes, NJ) and a computer station running Cell-Quest software (Becton Dickinson, Franklin Lakes, NJ).

4.7. Immunofluorescence

Immunostaining was performed as described previously [39]. Briefly, U251 cells were pretreated with compound 20 (1, 2, 4, 8, 16 and 20 μM) for 4 h, stimulated with 50 ng/ml TNFα for 30 min and then incubated at 4 °C overnight with p65 primary antibodies (1:200; Santa Cruz Biotechnology, Santa Cruz, CA). After washing with PBS, cells were incubated at 37 °C for 1 h with FITC–labeled secondary goat anti-mouse IgG antibodie. Cells were then stained with fluorochrome dye DAPI (Santa Cruz Biotechnology, Santa Cruz, CA) to visualize the cell nuclei, and observed under a fluorescence microscopy (OlympusIX51, Japan) with a peak excitation wave length of 340 nm.

4.8. Western-blot analysis

To determine the effect of GA on TNF-dependent IκBα phosphorylation, IκBα degradation, the U251 cells were serum-starved for 6 h and treated with GA for 4 h prior to the treatment of 50 ng/ml TNFα for different time periods and collected and lysed in lysis buffer (100 mM Tris-Cl, pH 6.8, 4% (m/v) sodium dodecylsulfonate, 20% (v/v) glycerol, 200 mM b-mercaptoethanol, 1 mM phenylmethylsulfonyl fluoride, and 1 g/mL aprotinin). Lysates were centrifuged at 12,000 g for 30 min at 4 °C. The concentration of total proteins was measured using the BCA assay method with Varioskan spectrofluorometer and spectrophotometer (Thermo, Waltham, MA) at 562 nm. The cytoplasmic and nuclear fractions were prepared as described above. Protein (20–100 μg) prepared from the indicated cells was loaded per lane and electrophoresed in 8% or 10% sodium dodecyl sulfate polyacrylamide gel electrophoresis (SDS-PAGE), and then transferred onto polyvinylidene difluoride (PVDF) Immobilon-P membrane (Bio-Rad, Hercules, CA) using a transblot apparatus (Bio-Rad, Hercules, CA). The membranes were blocked with 5% (w/v) non-fat milk at 30 min at 37 °C, followed by overnight incubation at 4 °C with primary antibodies diluted in PBST (1:2000 for β-actin; 1:500 for IκBα; 1:500 for p-IκBα (ser 32/36), Santa Cruz, CA). After washing with PBST, the membranes were incubated for 1 h with an IRDyeTM 800 conjugated secondary antibody diluted 1:20000 in PBST, and the labeled proteins were detected with an Odyssey Scanning System (LI-COR., Lincoln, Nebraska, USA).

4.9. IKKβ assay

12.5 μL of the 4 × reaction cocktail containing 50 ng IKKβ (supplied from the HTScan IKKβ kinase assay kit, Cell Signaling Technology, Beverly, MA) was incubated with 12.5 μL test sample for 5 min at room temperature. 25 μL 2 × ATP/substrate peptide cocktail was added to the preincubated reaction. After incubation at room temperature for 30 min, a 50 μL stop solution (50 mM EDTA, pH = 8) was added to stop the reaction. Then 25 μL of each reaction were transferred to a 96-well streptavidin-coated plate (PerkinElmer Life Sciences, Boston). After adding 75 μL dH_2O, the mixture was incubated at room temperature for 60 min. After thoroughly washing the wells 3 times with PBST, 100 μL primary antibody [Phospho-IκBα (Ser32) (14D4) Rabbit mAb, 1:1000 in PBS/T with 1% bovine serum albumin (BSA)] was added per well. After 120 min incubation at room temperature, the wells were thoroughly washed 3 times with PBST. 100 μL diluted HRP-labeled anti-rabbit IgG (1:1000 in PBS/T with 1% BSA) was added per well. After 30 min incubation at room temperature, the wells were washed five times with PBST. Then 100 μL TMB substrate was added into each well, and the plate was incubated at room temperature for 15 min. After adding the stop solution (100 μL/well), the plate was incubated at room temperature for 15 min and then read at 450 nm with Varioskan spectrofluorometer and spectrophotometer (Thermo, Waltham, MA).

Acknowledgments

This work was supported by the Project Program of State Key Laboratory of Natural Medicines, China Pharmaceutical University (No. JKGQ201103), 2008ZX09401-001 and 2009ZX09501-003 of National Major Science and Technology Project of China (Innovation and Development of New Drugs), 90713038 of National Natural Science Foundation of China (Key Program).

References

[1] Q.B. Han, H.X. Xu, Curr. Med. Chem. 16 (2009) 3775–3796.
[2] O. Chantarasriwong, A. Batova, W. Chavasiri, E.A. Theodorakis, Chem. Eur. J. 16 (2010) 9944–9962.
[3] X. Xu, Y. Liu, L. Wang, J. He, H. Zhang, X. Chen, Y. Li, J. Yang, J. Tao, Int. J. Dermatol. 48 (2009) 186–192.
[4] J.J. Rong, R. Hu, X.M. Song, J. Ha, N. Lu, Q.D. You, Q.L. Guo, Cancer Lett. 296 (2010) 55–64.
[5] Y. Qin, L. Meng, C. Hu, W. Duan, Z. Zuo, L. Lin, X. Zhang, J. Ding. Mol. Cancer Ther. 6 (2007) 2429–2440.
[6] J. Yu, Q.L. Guo, Q.D. You, L. Zhao, H.Y. Gu, Y. Yang, H.W. Zhang, Z. Tan, X. Wang, Carcinogenesis 28 (2007) 632–638.
[7] T.W. Zhou, Phase I human tolerability trial of gambogic acid, Chin. J. New Drugs 16 (2007) 79–82.
[8] L. Zhao, Q.L. Guo, Q.D. You, Z.Q. Wu, H.Y. Gu, Biol. Pharm. Bull. 27 (2004) 998–1003.

[9] Q. Zhao, Y. Yang, J. Yu, Q.D. You, S. Zeng, H.Y. Gu, N. Lu, Q. Qi, W. Liu, X.T. Wang, Q.L. Guo, Cancer Lett. 262 (2008) 223–231.
[10] Q.L. Guo, S.S. Lin, Q.D. You, H.Y. Gu, J. Yu, L. Zhao, Q. Qi, F. Liang, Z. Tan, X. Wang, Life Sci. 78 (2006) 1238–1245.
[11] T. Yi, Z. Yi, S.G. Cho, J. Luo, M.K. Pandey, B.B. Aggarwal, M. Liu, Gambogic acid inhibits angiogenesis and prostate tumor growth by suppressing vascular endothelial growth factor receptor 2 signaling, Cancer Res. 68 (2008) 1843–1850.
[12] N. Lu, Y. Yang, Q.D. You, Y. Ling, Y. Gao, H.Y. Gu, L. Zhao, X.T. Wang, Q.L. Guo, Cancer Lett. 258 (2007) 80–89.
[13] F. Nie, X. Zhang, Q. Qi, L. Yang, Y. Yang, W. Liu, N. Lu, Z. Wu, Q. You, Q. Guo, Toxicology 260 (2009) 60–67.
[14] Y.C. Xin, Q.B. Han, C.Y. Chan, H. Wang, Z. Liu, D.T.Y. Christopher, H.K. Cheng, H.X. Xu, Proteomics 9 (2009) 242–253.
[15] M.K. Pandey, B. Sung, K.S. Ahn, A.B. Kunnumakkara, M.M. Chaturvedi, B.B. Aggarwal, Blood 110 (2007) 3517–3525.
[16] U.D. Palempalli, U. Gandhi, P. Kalantari, H. Vunta, R.J. Arner, V. Narayan, A. Ravindran, K.S. Prabhu, Biochem. J. 419 (2009) 401–409.
[17] S. Kasibhatla, A. Jessen Katayoun, S. Maliartchouk, Y.W. Jean, M.E. Nicole, J. Drewe, L. Qiu, P.A. Shannon, E.P. Anthony, N. Sirisoma, S. Jiang, H.Z. Zhang, R.G. Kurt, X.C. Sui, R.G. Douglas, B. Tseng, Proc. Natl. Acad. Sci. U.S.A. 102 (2005) 12095–12100.
[18] E. Suzuki, T.R. Daniels, G. Helguera, M.L. Penichet, K. Umezawa, B. Bonavida, Inhibition of NF-kappaB and Akt pathways by an antibody-avidin fusion protein sensitizes malignant B-cells to cisplatin-induced apoptosis, Int. J. Oncol. 36 (2010) 1299–1307.
[19] F. Chen, V. Castranova, X. Shi, L.M. Demers, Clin. Chem. 45 (1999) 7–17.
[20] S. Ghosh, Immunol. Res. 19 (1999) 183–189.
[21] E.N. Hatada, D. Krappmann, C. Scheidereit, Curr. Opin. Immunol. 12 (2000) 52–58.
[22] S. Ghosh, M. Karin, Cell 109 (Suppl) (2002) S81–S96.
[23] O. Chantarasriwong, W.C. Cho, A. Batova, W. Chavasiri, C. Moore, A.L. Rheingold, E.A. Theodorakis, Org. Biomol. Chem.(7) (2009) 4886–4894.
[24] X.J. Wang, N. Lu, Q. Yang, D. Gong, C.J. Lin, S.L. Zhang, M.Y. Xi, Y. Gao, L.B. Wei, Q.L. Guo, Q.D. You, Eur. J. Med. Chem. 46 (2011) 1280–1290.
[25] E. Niederberger, G. Geisslinger, FASEB J. 22 (2008) 3432–3442.
[26] S. Nagarajan, M. Doddareddy, H. Choo, Y.S. Cho, K.S. Oh, B.H. Lee, A.N. Pae, Bioorg. Med. Chem. 17 (2009) 2759–2766.
[27] H.P. Sun, J. Zhu, F.H. Chen, S.L. Zhang, Y. Zhang, Q.D. You, Eur. J. Med. Chem. 46 (2011) 3942–3952.
[28] A. Baxter, S. Brough, A. Cooper, E. Floettmann, S. Foster, C. Harding, J. Kettle, T. McInally, C. Martin, M. Mobbs, M. Needham, P. Newham, S. Paine, S. St-Gallay, S. Salter, J. Unitt, Y. Xue, Bioorg. Med. Chem. Lett. 14 (2004) 2817–2822.
[29] T. Morwick, A. Berry, J. Brickwood, M. Cardozo, K. Catron, M. DeTuri, J. Emeigh, C. Homon, M. Hrapchak, S. Jacober, S. Jakes, P. Kaplita, T.A. Kelly, J. Ksiazek, M. Liuzzi, R. Magolda, C. Mao, D. Marshall, D. McNeil, A. Prokopowicz 3rd, C. Sarko, E. Scouten, C. Sledziona, S. Sun, J. Watrous, J.P. Wu, C.L. Cywin, J. Med. Chem. 49 (2006) 2898–2908.
[30] J.A. Christopher, P. Bamborough, C. Alder, A. Campbell, G.J. Cutler, K. Down, A.M. Hamadi, A.M. Jolly, J.K. Kerns, F.S. Lucas, G.W. Mellor, D.D. Miller, M.A. Morse, K.D. Pancholi, W. Rumsey, Y.E. Solanke, R. Williamson, J. Med. Chem. 52 (2009) 3098–3102.
[31] A.H. Bingham, R.J. Davenport, R. Fosbeary, L. Gowers, R.L. Knight, C. Lowe, D.A. Owen, D.M. Parry, W.R. Pitt, Bioorg. Med. Chem. Lett. 18 (2008) 3622–3627.
[32] J.A. Christopher, B.G. Avitabile, P. Bamborough, A.C. Champigny, G.J. Cutler, S.L. Dyos, K.G. Grace, J.K. Kerns, J.D. Kitson, G.W. Mellor, J.V. Morey, M.A. Morse, C.F. O'Malley, C.B. Patel, N. Probst, W. Rumsey, C.A. Smith, M.J. Wilson, Bioorg. Med. Chem. Lett. 17 (2007) 3972–3977.
[33] A.H. Bingham, R.J. Davenport, L. Gowers, R.L. Knight, C. Lowe, D.A. Owen, D.M. Parry, W.R. Pitt, Bioorg. Med. Chem. Lett. 14 (2004) 409–412.
[34] Q. L. Guo. Q. D. You, F. Feng, W. Y. Liu, Chinese Patent ZL01008049 (2003).
[35] E.J. Tisdale, I. Slobodov, E.A. Theodorakis, Org. Biomol. Chem. 1 (2003) 4418–4422.
[36] N.G. Li, X.R. Liu, C.J. Lin, Q.D. You, Tetrahedron Lett. 48 (2007) 6586–6589.
[37] Z.Q. Wu, Q.L. Guo, Q.D. You, L. Zhao, H.Y. Gu, Biol. Pharm. Bull. 27 (2004) 1769–1774.
[38] Y. Hu, Y. Yang, Q.D. You, W. Liu, H.Y. Gu, L. Zhao, K. Zhang, W. Wang, X.T. Wang, Q.L. Guo, Biochem. Biophys. Res. Commun. 351 (2006) 521–527.
[39] S.A. Reddy, M.M. Chaturvedi, B.G. Darnay, H. Chan, M. Higuchi, B.B. Aggarwal, J. Biol. Chem. 269 (1994) 25369–25372.
[40] T. Kondo, T. Setoguchi, T. Taga, Proc. Natl. Acad. Sci. U. S. A 101 (2004) 781–786.
[41] G. Xu, Y.C. Lo, G. Napolitano, X. Wu, X. Jiang, M. Dreano, M. Karin, H. Wu, Nature 472 (2011) 325–330.